



CHALMERS



An investigation of foaming properties of the hemicellulose galactoglucomannan

Master's thesis in Materials Chemistry

JESSICA FREDRIKSSON

Department of Chemistry and Chemical Engineering

CHALMERS UNIVERSITY OF TECHNOLOGY

Gothenburg, Sweden 2018

Master's thesis 2018

AN INVESTIGATION OF THE FOAMING PROPERTIES OF THE
HEMICELLULOSE GALACTOGLUCOMANNAN

JESSICA FREDRIKSSON



Department of Chemistry and Chemical Engineering

Division of Applied Chemistry

Pharmaceutical Technology

Chalmers University of Technology

Gothenburg, Sweden 2018

An investigation of foaming properties of the hemicellulose
galactoglucomannan

© JESSICA FREDRIKSSON, 2018

Examiner: Anette Larsson, Chemistry and Chemical Engineering

Master's Thesis 2018

Department of Chemistry and Chemical Engineering

Division of Applied Chemistry

Pharmaceutical Technology

Chalmers University of Technology

SE-412 96 Gothenburg

Telephone +46 31772 10 00

Cover: Siphon foaming of galactoglucomannan modified with divinyl sulfone
and butyl glycidyl ether, mixed with nanofibrillated cellulose.

An investigation of foaming properties of the hemicellulose galactoglucomannan

JESSICA FREDRIKSSON

Department of Chemistry and Chemical Engineering

Chalmers University of Technology

Abstract

In modern society, sustainable thinking together with environmentally friendly aspects are essential. Hence, turning useless by-products to substances of importance is of great interest. The hemicellulose galactoglucomannan is such a by-product and can be found in the process water from pulp manufacturing. The aim of this master thesis project is therefore to investigate the foaming ability of galactoglucomannan. Beforehand, the hemicellulose needs to be extracted from the process water and therefore an optimisation procedure where the hemicellulose was extracted with different concentration of ethanol was performed. The different extracted hemicelluloses were characterised, and some variation in carbohydrate content, molecular weight, and functional groups could be seen. The hemicellulose requires modifications to improve the foaming properties. This was done by introducing hydrophobic side groups, using butyl glycidyl ether, to the structure for increasing the hydrophobic nature, but also introducing chain extension, using divinyl sulfone as the agent, in order to increase the molecular weight. The modifications were successfully made and confirmed with surface activity test together with infrared analysis, thermogravimetric analysis and differential scanning calorimetry. The foaming procedure was made using a siphon, and the result indicated that galactoglucomannan based materials can generate a foam. The unmodified and the more hydrophobic galactoglucomannan both produced a foam, but not the crosslinked sample. The hydrophobic sample generated a more stable foam, and with addition of nanofibrillated cellulose the stability of the foam was even higher. However, the stability is still a limitation and the foam structure broke down after a short time. Therefore, the stability of the foams requires further investigations.

Keywords: Foam, siphon, hemicellulose, galactoglucomannan, nanofibrillated cellulose, butyl glycidyl ether, divinyl sulfone.

Acknowledgement

The master thesis project has been carried out at the division of applied chemistry at Chalmers University of Technology during the spring of 2018. I want to express a special gratitude to Anette Larson, who has been my examiner and guiding star. The project would not have been possible without the help of Robin Nilsson and I owe him a big thank you. I also want to thank everyone in the group pharmaceutical technology, and the other students that I shared office with during the project work, thanks for all the support and laughs. Lastly, I want to show my appreciation to my family and friends, and especially to Linnea Viklund for all your assistance!

Jessica Fredriksson, Gothenburg, June 2018

Table of Contents

List of Figures	xi
List of Tables.....	xii
1. Introduction	2
2. Theoretical background.....	4
2.1 Wood	4
2.1.1 Cellulose	5
2.1.2 Lignin.....	5
2.1.3 Hemicellulose	5
2.1.4 Galactoglucomannan (GGM).....	6
2.2 Polymeric foams and manufacturing	6
2.2.1 The siphon method for generating polymeric foams	7
2.2.2 Hot-mould baking for generating polymeric foams.....	7
2.3 Modifications of GGM for enabling foam manufacturing	7
2.3.1 Increase the hydrophobicity of GGM	8
2.3.2 Increase the molecular weight of GGM.....	8
3. Method	9
3.1 Extraction of GGM	9
3.2 Modification reactions of GGM	10
3.2.1 Introducing hydrophobic side chains to GGM.....	10
3.2.2 Introducing crosslinks to GGM for increasing the molecular weight.....	11
3.2.3 Introducing hydrophobic side chains to the crosslinked GGM	12
3.3 Characterisation analysis	12
3.3.1 Carbohydrate analysis	12
3.3.2 Ultraviolet-visible (UV vis) spectroscopy	12
3.3.3 Size exclusion chromatography (SEC)	12
3.3.4 Fourier-transform infrared (FTIR) spectroscopy	13
3.3.5 Pendant drop analysis	13
3.3.6 Thermogravimetric analysis (TGA).....	13
3.3.7 Differential scanning calorimetry (DSC).....	13
3.3.8 Attenuated total reflection Fourier-transform infrared spectroscopy (ATR-FTIR)13	
3.4 Siphon foaming.....	13

3.5	Hot-mould baking foam method.....	14
4.	Results and Discussion.....	15
4.1	Characterisation of the extracted GGM.....	15
4.2	Analysis of the modifications of GGM	19
4.3	Results from the siphon foaming experiments	24
4.4	Result from the initial step for the hot-mould baking foam method	25
5.	Conclusion and Future Outlook	27
	References	29
	Appendix	II
	Appendix A - Protocols.....	II
A.1	Extraction procedure.....	II
A.2	Crosslinking procedure optimisation.....	III
A.3	Protocol for introducing hydrophobic side chains to the GGM	III
A.4	Protocol for introducing crosslinks to GGM for increasing the molecular weight ...	IV
A.5	Protocol for introducing hydrophobic side chains to the crosslinked GGM	IV
A.6	Protocol for the carbohydrate analysis	IV
	Appendix B – Results.....	V
B.1	Result from the carbohydrate analysis for the ethanol extracted GGM	VI
B.2	Lignin content for the ethanol extracted GGM	VI
B.3	Result from the SEC analysis of the ethanol extracted GGM	VII
B.4	FTIR result for the ethanol extracted GGM	VII
B.5	DSC calculations	X
B.6	Result from the siphon foaming	XI

List of Figures

Figure 1. Structure of the glucose monomer, building up the cellulose molecule.	5
Figure 2. Representative structure of the GGM molecule, with mannose and glucose in the backbone, galactose in side chain, and acetyl groups (Ac).	6
Figure 3. Reaction scheme over the introduction of hydrophobic side chains, using BGE, to the GGM structure, represented by a monosaccharide unit. The acetyl group (Ac) cleaves with alkali treatment (NaOH).	10
Figure 4. Reaction scheme over the introduction of crosslinks using DVS to the GGM structure, represented by monosaccharide units. The acetyl group (Ac) cleaves with alkali treatment (NaOH).	11
Figure 5. The yield of the precipitations from the ethanol extraction experiments in relation to the concentration of the ethanol.	16
Figure 6. The infrared spectra from the FTIR analysis for the ethanol extracted GGMs.	18
Figure 7. The surface tension results from the pendent drop analysis for the modified GGMs and an unmodified as reference.	20
Figure 8. The result from TGA analysis for the modified GGMs and an unmodified as reference.	20
Figure 9. The result from DSC analysis, heating range -60°C to 200°C, for the modified GGMs and an unmodified as reference. The peaks correspond to water evaporation.	21
Figure 10. The ATR-FTIR spectra for the modified GGMs and an unmodified as reference.	22
Figure 11. Result from the siphon foaming experiments showing the percentage of foam in relation to the total sample volume as function of time after the foaming procedure. GGM-DVS represents all the foaming experiments with the DVS modified GGM, even the one mixed with NFC, since none of them generated a foam. The sample for GGM (30% (w/w)) is not represented, since it did not generate a foam.	24
Figure 12. Result from the siphon foaming experiments showing the percentage of foam in relation to initial foam volume as function of time after the foaming procedure. GGM-DVS represents all the foaming experiments with the DVS modified GGM, even the one mixed with NFC, since none of them generated a foam. The sample for GGM (30% (w/w)) is not represented, since it did not generate a foam.	25
Figure 13. Results from the initial step for the hot-mould baking foam method, temperature of 150°C and holding time of 5 minutes. Left to right, GGM-DVS, GGM-BGE, GGM-DVS-BGE.	26
Figure B. 1. FTIR spectra for the 1:1 ethanol extracted GGM samples.	VII
Figure B. 2. FTIR spectra for the 1:2 ethanol extracted GGM samples.	VIII
Figure B. 3. FTIR spectra for the 1:1.5 ethanol extracted GGM samples.	VIII
Figure B. 4. FTIR spectra for the 1:3 ethanol extracted GGM samples.	IX
Figure B. 5. FTIR spectra for the 1:2.5 ethanol extracted GGM samples.	IX

List of Tables

Table 1. The solutions, including the initial GGM and NFC slurry content, used for the siphon foaming experiments.	14
Table 2. The samples and conditions used for the initial step for the hot-mould baking foam method.	14
Table 3. Result from the carbohydrate analysis, showing the ratio of galactose, glucose, and mannose content for the different ethanol extracted GGMs. The data is an average of the two replicates for each ethanol concentration.	17
Table 4. The acid soluble lignin content and the Klason lignin content in percentage of the total mass of the precipitate for the ethanol extracted GGMs as average of the two replicates for each ethanol concentration.	17
Table 5. The result from the SEC analysis, the values together with the uncertainty for the number-average molecular weight (Mn), the weight-average molecular weight (Mw), and the polydispersity (Mw/Mn) as average of the two replicates for each ethanol concentration, are displayed for the different ethanol extracted GGMs.	18
Table 6. The absorption bands at $\sim 3400\text{ cm}^{-1}$, $\sim 1750\text{ cm}^{-1}$, and $\sim 1250\text{ cm}^{-1}$ from the FTIR for the ethanol extracted GGMs, and the ratio between these absorption bands.	19
Table 7. The absorption bands at $\sim 2900\text{ cm}^{-1}$, and $\sim 1250\text{ cm}^{-1}$ from the ATR-FTIR for the modified GGMs with an unmodified as reference, and the ratio between these absorption bands.	23
Table A. 1. Different amount of ethanol (95%) and refined process water generating different ratios for the extraction procedure.	II
Table A. 2. The GGM solutions, crosslinking agents, and ratio of GGM to crosslinking, that were varied for the crosslinking procedure optimisation.	III
Table B. 1. The result from the carbohydrate analysis, which shows the monosaccharides content of the different ethanol extracted GGMs.	VI
Table B. 2. The acid soluble lignin content and the Klason lignin content in percentage of the total mass of the precipitate for the ethanol extracted GGMs.	VI
Table B. 3. The result from the SEC analysis for the ethanol extracted GGMs. Showing the number-average molecular weight (Mn), the weight-average molecular weight (Mw), and the polydispersity (Mw/Mn), the uncertainty weighted radius average ($r(\text{avg})$), the hydrodynamic radius ($r_h(v)$), the injected mass, the calculated mass, the mass fraction, the mass recovery, the peak range, and the weight-average intrinsic viscosity ($[\eta]w$). The results are averaged of the two replicates for each ethanol concentration.	VII
Table B. 4. Siphon foaming experiment using GGM (30% (w/w)) mixed with NFC slurry (10% (w/w)). Showing the amount of the different components used and the mass used in the siphon. Since it did not foam, no mass, volume or density could be measured.	XI
Table B. 5. Siphon foaming experiment using GGM (5% (w/w)) mixed with NFC slurry (10.5% (w/w)). Showing the amount of the different components used and the mass used in	

the siphon, the mass and volume direct after the foaming, as well as the calculated density of the wet foam. Moreover, picture from direct after the foaming and 5 minutes later.	XI
Table B. 6. Siphon foaming experiment using GGM-BGE (5.91% (w/w)). Showing the mass of the solution used in the siphon, the mass and volume direct after the foaming, as well as the calculated density of the wet foam. Moreover, pictures from direct after the foaming, 5 minutes later, 30 minutes later and 60 minutes later.	XII
Table B. 7. Siphon foaming experiment using GGM-BGE (5.91% (w/w)) mixed with NFC slurry (11% (w/w)). Showing the amount of the different components used and the mass used in the siphon, the mass and volume direct after the foaming, as well as the calculated density of the wet foam. Moreover, pictures from direct after the foaming, 5 minutes later, 30 minutes later and 60 minutes later.	XIII
Table B. 8. Siphon foaming experiment using GGM-DVS (5% (w/w)). Showing the mass of the solution used in the siphon, the mass and volume direct after the foaming, as well as the calculated density of the wet foam. Moreover, pictures from direct after the foaming and 5 minutes later. No cellular structure, foam, is displayed.	XIV
Table B. 9. Siphon foaming experiment using GGM-DVS (5% (w/w)) diluted with milliQ water generating a 4.28% (w/w). Showing the mass of the different components, the mass of the solution used in the siphon, the mass and volume direct after the foaming, as well as the calculated density of the wet foam. Moreover, pictures from direct after the foaming and 5 minutes later. No cellular structure, foam, is displayed.	XV
Table B. 10. Siphon foaming experiment using GGM-DVS (4.28% (w/w)) mixed with GGM-DVS (5% (w/w)) generating a 4.32% (w/w), and the double amount of gas patrons as the other experiments. Showing the mass of the different components, the mass of the solution used in the siphon, the mass and volume direct after the foaming, as well as the calculated density of the wet foam. Moreover, pictures from direct after the foaming and 5 minutes later. No cellular structure, foam, is displayed.	XVI
Table B. 11. Siphon foaming experiment using GGM-DVS (4.32% (w/w)) mixed with NFC slurry (11% (w/w)). Showing the mass of the different components, the mass of the solution used in the siphon, the mass and volume direct after the foaming, as well as the calculated density of the wet foam. Moreover, pictures from direct after the foaming, 5 minutes later, 30 minutes later and 60 minutes later. No cellular structure, foam, is displayed.	XVII
Table B. 12. Siphon foaming experiment using GGM-DVS-BGE (4.79% (w/w)). Showing the mass of the solution used in the siphon, the mass and volume direct after the foaming, as well as the calculated density of the wet foam. Moreover, pictures from direct after the foaming, 5 minutes later, 30 minutes later and 60 minutes later.	XVIII
Table B. 13. Siphon foaming experiment using GGM-DVS-BGE (4.79% (w/w)) mixed with NFC slurry (10% (w/w)). Showing the amount of the different components used and the mass used in the siphon, the mass and volume direct after the foaming, as well as the calculated density of the wet foam. Moreover, pictures from direct after the foaming, 5 minutes later, 30 minutes later and 60 minutes later.	XIX

1. Introduction

Sustainability, material efficiency and utilisation are key concepts in the modern society. The importance of decreasing waste generation forms ambitions to find new areas of application for otherwise useless substances. This generates a driving force to investigate waste and useless by-products in different industries. One major industry, especially in Sweden, is the pulp and paper industry, in which wood is one of the main raw materials used(1). The pulp and paper industry generates several streams of waste during the production process. In this aspect, making use of the substances in these waste stream lines by finding new areas of usage would be of great interest.

The major parts of wood are cellulose, lignin, and hemicellulose(2). Processing of wood can generate different types of pulp depending on the source and the processing method used. Common for the processes are that the different elements in the material are dissolved or degraded, resulting in streams of by-products. The streams consist of several components, among these are hemicelluloses. The different components can be extracted using different methods, for example can certain hemicelluloses be extracted using alkali treatment. During production of pulp, a specific hemicellulose galactoglucomannan (GGM) is considered a by-product with no use as material and can be found in the process water. Hence, finding an area where GGM can be used would therefore be of gain in a sustainability aspect. One application area investigated in this master thesis project is in production of a polymeric foam.

Foamed materials are of interest since they are light-weight but still have a high modulus in relation to their weight(3). This property has generated a large amount of application areas for foamed materials, for example as packaging materials. The foaming process involves nucleation and bubble growth, generating a cell structure with gaseous voids. Within foam manufacturing, different factors affect the outcome product. This includes process pathway and blowing agents(4), where the blowing agents are required for creating the gaseous voids. The properties of the polymer will be important for the process pathway strategy, meaning that generating a foam with good porosity and density will depend on the polymeric characteristics connected to the foaming method.

The aim of this master thesis project is to investigate the possibility of GGM to be used in foam production. As has been mentioned, the GGM can be found in stream lines of process water from pulp manufacturing and therefore the initial step will be to extract the polymer from the water. The focus will be on utilising GGM from thermomechanical pulp (TMP) water that has been produced from softwood such as spruce. It has been established that from TMP water, GGM will precipitate in ethanol(5). However, since the alcohol can be hard to remove and in order to make the procedure more environmentally friendly, as small amount as possible is favourable and therefore this method will be optimised in a series of experiments.

To enable foam production, the GGM needs chemical modifications to obtain more favourable properties. Presenting side chains or chain extensions is expected to improve the foaming properties of the GGM. This by connecting hydrophobic side chains to the GGM molecules or by connecting the GGM molecules to generate longer molecular chains, thus increasing the hydrophobic nature of the molecule and increasing the molecular weight, which will be favourable for creating thermoplastic properties.

The process of producing a foam will, still at a low scale, be performed with large scale production in mind. This means that the design of the procedure will consider economical and sustainable aspects, as well as energy efficiency. In the manufacturing, blowing agents will be used for generation of the cellular structure. The blowing agents will be substances that are advantageous in an environmentally friendly aspect, such as water and baking soda. The purpose with the project is to see if foam can be produced using GGM or modifications of GGM.

2.

Theoretical background

This chapter aims to provide a better understanding of the project by presenting the topics in focus, including the raw material from which the centre polymer is received and the different modifications that enables better usage of it. Moreover, the methods of producing polymeric foams will be presented.

2.1 Wood

Wood is a naturally occurring hierarchically structured material(6), where the dominating components are cellulose, lignin, and hemicellulose(2). The hierarchical structure of wood enables different properties and functions at each level, generating a variety of applications.

Wood is used as raw material in several areas, where a main one is in the pulp and paper industry. The pulp is used for example in producing different types of paper, cardboard packaging, and paper towels(7). The different components of wood are separated in the pulping process, which can be chemical, semi-chemical or mechanical. One type of mechanical pulp is the thermomechanical pulp (TMP), in which the milling take place under high temperature(8). The properties of the pulps vary depending on the pulping process and the wood species used(9). Wood can generally be categorised into hardwood and softwood,

both of which have variations in structural and chemical composition(5). The softwood species, gymnosperms, have their seeds in an open environment where they are said to be naked(10). On the contrary, the hardwood species, angiosperms, have their seed in an enclosed environment(11).

2.1.1 Cellulose

Cellulose is the main component in the cell walls of plants, where it has the function of mechanical support, and is insoluble in most solvents(2). The cellulose molecule is built up by glucose monomers, forming a linear structure, see Figure 1. The glucose monomers have the tendency to form hydrogen bonds and self-assembly into microfibrils(2). Depending on how the microfibrils align themselves, the degree of crystallinity varies. The microfibrils will further self-assembly into fibrils and then eventually into the cellulose fibre. This process generates the hierarch nature of the cellulose molecules.

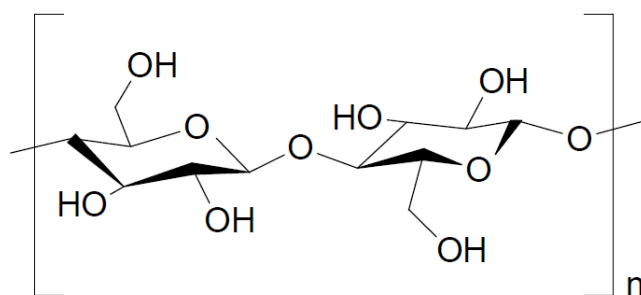


Figure 1. Structure of the glucose monomer, building up the cellulose molecule.

2.1.2 Lignin

The lignin molecule has a random structure(12) and is an amorphous polymer with hydroxylated phenylpropane units(2). In wood, the lignin act as a reinforcer. Two types of lignin are of importance, the Klason lignin and the acid-soluble lignin. The Klason lignin can be separated by initial treatment with strong sulfuric acid, followed by heating. This treatment will cause the polysaccharides to hydrolyse and dissolve, but the Klason lignin will remain solid. The solid Klason lignin residue can be filtrated and collected. The acid-soluble lignin needs to be accounted for in other ways since it will dissolve in the hydrolysis process. The amount of acid-soluble lignin in the sample can be analysed using UV spectrophotometry at 200-205 nm, which is where the acid-soluble lignin has its maximum absorption(2).

2.1.3 Hemicellulose

Hemicelluloses are, in general, heteropolysaccharides, found between the cellulose fibrils in the cell wall(9). They are categorised into groups depending on the polysaccharide content which differs depending on the origin. The main groups are xylans, mannoglycans, xyloglucans, and mixed-linkage beta-glucans(13). The different types of hemicelluloses have variations in side chains, distribution, and in the glycoside linkage in the main chains, giving them different properties.

The mannoglycans are further divided into galactomannans, glucomannans, and galactoglucomannans depending on the backbone composition(13). The galactomannans have a backbone consisting of mannose. Glucomannans and galactoglucomannans both have backbones consisting of mannose and glucose, but galactoglucomannans also have side chains of galactose.

2.1.4 Galactoglucomannan (GGM)

The hemicellulose galactoglucomannan (GGM) is composed of a backbone consisting of (1→4)-mannose and (1→4)-glucose with connecting side groups of (1→6)-galactose(14), see Figure 2. The GGM can be found in both softwood and hardwood species, most commonly in softwood where the ratio of the monosaccharides differs from the ratio 0.1 galactose:1 glucose:3-4 mannose to the ratio 1 galactose:1 glucose:3-4 mannose(9). The water solubility of GGM is affected by the galactose content, where less galactose units in the structure of the GGM will exhibit lower water solubility. In addition, acetyl groups are often attached to the mannose residue in the GGM structure. However, these can be cleaved under alkali treatment(9),(15). The processing of softwood species generates waste streams consisting of GGM. In mechanical pulp from softwood, the dominating hemicellulose is the acetylated GGM(2). The streams will contain more than the GGM molecules and therefore the streams need further processing for generation of pure GGM(16).

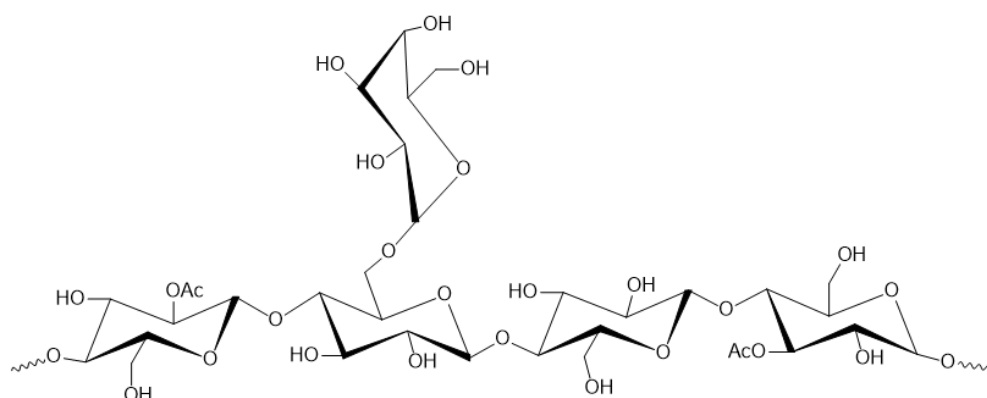


Figure 2. Representative structure of the GGM molecule, with mannose and glucose in the backbone, galactose in side chain, and acetyl groups (Ac).

2.2 Polymeric foams and manufacturing

Production of a polymeric foam can be performed in a range of methods and with different starting materials. The interest and the discovery of foams is due to the advantage in using foams instead of other structured materials. The foams are light-weight but still possess high strength(6). Depending on if the structure is open or closed, wet or dry, the properties and with that the applications, will differ.

The structure of the foam arises from the formation of gas bubbles that will grow and generate the cellular structure(6), making the bubble generation an important feature in the foam formulation procedure. Blowing agents are used to generate the bubbles and therefore

choosing the blowing agents, including the interaction of the blowing agents with the polymer solution, is a crucial factor. The performance of the blowing agents varies, some can be decomposed in the polymer material and release gas that will generate the bubbles, which is the case for sodium bicarbonate. However, this will leave some residue of the blowing agent in the produced foam. To avoid this, water or carbon dioxide can be used. These will expand when pressure is released and that will generate a structure with no trace of the blowing agent, which is advantageous when the foam is used for food packaging or medical substances(6).

For the foam to be useful, the stability is an essential factor. A method for increasing the stability is usage of a stabiliser, which can be nanofibrillated cellulose (NFC)(17). The cellulose residue is 4 nm in width and 500-1000 nm in length(17) and when mixed with the polymer solution and upon foaming, the fibrils can arrange at the interface of the bubble or increase the viscosity of the solution between the bubbles, and with that stabilise the foam structure.

2.2.1 The siphon method for generating polymeric foams

A method for generating polymeric foam is by using a siphon. The polymer solution in the siphon will be introduced to nitrous oxide gas. The apparatus will be shaken, distributing the gas in the liquid. Introducing the gas, the pressure in the siphon will increase and when the pressure is reduced again, by opening the nozzle, the gas will leave the solution, creating bubbles. This will generate the foam structure.

Nitrous oxide dissolves better than, for example, carbon dioxide in hydrocarbons(18). This enables better distribution in fatty solutions, hence, the nitrous gases are used in whipping of creams, the traditional usage of the siphon.

2.2.2 Hot-mould baking for generating polymeric foams

Using pressuring plates is also a way to generate the foam structure(19). The polymer solution is placed between two hot plates, where the temperature is set. The upper plate generates pressure and the water in the solution will act as a blowing agent. The water will evaporate, and when the pressure is released the foam structure will appear.

2.3 Modifications of GGM for enabling foam manufacturing

The GGM molecule needs, as mentioned, to undergo modifications for changing the properties in respect to the hydrophobicity and the molecular weight. The modifications can be confirmed with different analysis techniques, such as infrared spectroscopy and pendant drop analysis. In infrared spectroscopy, the change in the functional groups is analysed and some important signals when analysing modified GGM could be from the acetyl groups ($\sim 1700\text{ cm}^{-1}$), the hydroxy groups ($\sim 3400\text{ cm}^{-1}$), and the ether linkage ($\sim 1200\text{ cm}^{-1}$) between the saccharide units(20).

2.3.1 Increase the hydrophobicity of GGM

The GGM molecule is water soluble(21)(22). Modifying the polymer with hydrophobic chains will increase the hydrophobic nature of the polymer, which will decrease the water solubility(23). The modified molecule will contain both hydrophobic and hydrophilic areas and this amphiphilic nature will make it surface active.

Hydrophobic modifications can be done using different agents. These need to exhibit reactive sites that can react with the hydroxy groups on the GGM molecule. Since epoxy groups are highly reactive(24), an epoxy resin can be used for the purpose of attaching hydrophobic side chains to the polymer chain.

2.3.2 Increase the molecular weight of GGM

Crosslinking of polymers can be done either by chemical bonding or physical interactions(25). The chemical bonding procedure can be performed during or after polymerisation. The post-polymerisation crosslinking often requires a crosslinking agent, which interacts with reactive groups on the polymer chain. All crosslinking reactions need promotion, which usually comes from heating or photoirradiation. The chemically crosslinked polymers form a network and if the crosslinking have strong interactions they will decompose instead of melt when heated. The physical crosslinking can form reversible networks, meaning the bonding is not permanent.

Similar reagents as for crosslinking can be used to partly bind some GGM molecules together to increase the molecular weight of GGM, where the crosslinker is preferred to interact with the hydroxy groups at the end of the chains to get almost linear polymer chains of increased molecular weight. An increased molecular weight can be achieved by using a molecule with an epoxy group at each end of the molecule. The two-sided epoxy resin would generate longer GGM chains, since it would act as an anchor connecting the GGM chains.

3.

Method

The initial step in the project was to extract GGM with ethanol from refined process water. This was performed with a procedure to find the optimal ratio of ethanol, which was later used for obtaining the GGM for further modifications. The dried extracted GGMs were analysed in respect to their carbohydrate content, acid soluble lignin content, Klason lignin content, and their molecular weight was investigated together with the functional groups.

Two different modification reactions were performed on the extracted GGM, one introducing hydrophobic side chains, and one extending the GGM molecules. The modifications were confirmed by analysis of the functional groups, the surface activity, and the thermal behaviour.

The last step in the project was foaming, which was performed with two different methods, siphon foaming and an initial step for hot-mould bake foaming.

3.1 Extraction of GGM

Membrane filtrated process water from manufacturing of thermomechanical pulp containing 4% (w/w) was received from Stora Enso. Different rations, from 0.5 part ethanol (95%) to one part process water up to 3 parts ethanol to one part process water, were added to the process

water to precipitate the GGM, see Table A. 1 in Appendix A.1. The mixture was stirred for approximately 3 hours in room temperature, before they were centrifuged (Sigma 4K15, speed 5100, RCF 5525, 15 minutes) and the precipitations were transferred to petri dishes for drying in room temperature.

3.2 Modification reactions of GGM

Three different reaction procedures were performed, GGM modified by introducing hydrophobic side chains using butyl glycidyl ether (BGE), GGM modified by introducing crosslinks using the crosslinking agent divinyl sulfone (DVS), and GGM modified with both DVS and BGE. The procedures were performed similar to Nypelö et al.(23), and Peresin et al.(26).

3.2.1 Introducing hydrophobic side chains to GGM

For protocol of the procedure, see Appendix A.3. NaOH pellets were added to ~200 g 10% (w/w) GGM solution in mole equivalent of 3:1 NaOH to GGM monomer. After dissolution, BGE in mole equivalent of 3:1 BGE to GGM monomer was added and the solution stood overnight in a 45°C oil bath and with stirring at 730 ppm. The solution was then neutralised and dialysed for approximately one week. The expected scheme over the reaction can be seen in Figure 3.

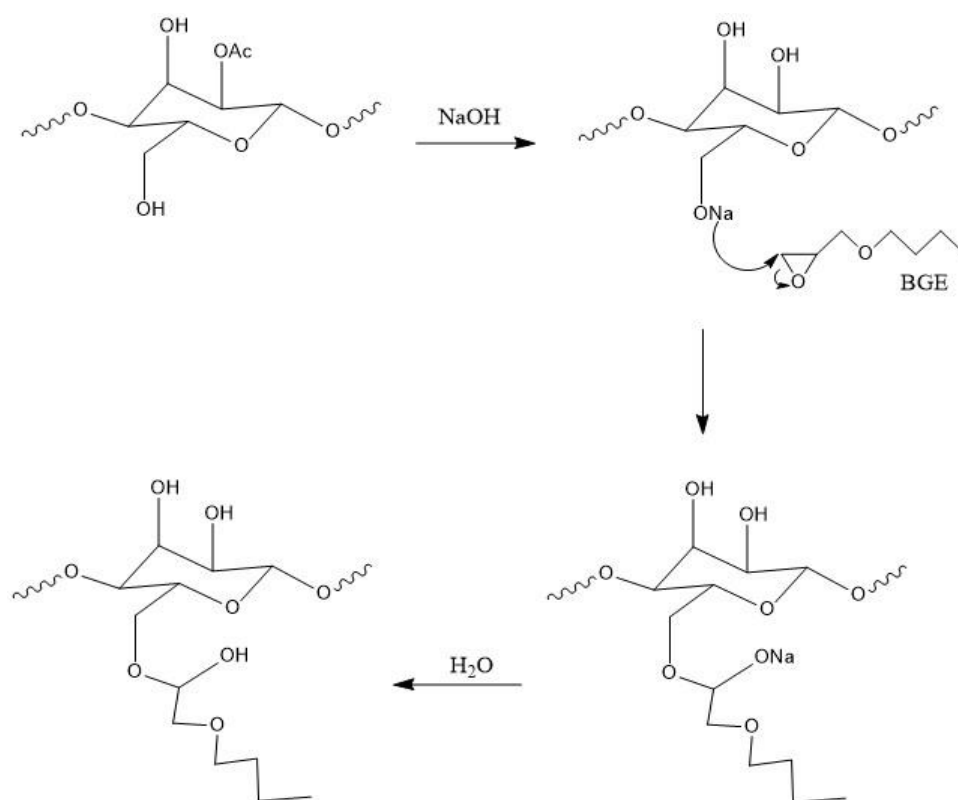


Figure 3. Reaction scheme over the introduction of hydrophobic side chains, using BGE, to the GGM structure, represented by a monosaccharide unit. The acetyl group (Ac) cleaves with alkali treatment (NaOH).

3.2.2 Introducing crosslinks to GGM for increasing the molecular weight

The crosslinking reaction was initially performed in an optimising procedure by usage of different crosslinking agents and conditions, see Appendix A.2, before the final reaction pathway was chosen, which is described here. For protocol of the final pathway, see Appendix A.4. NaOH pellets were added to ~600 g 5% (w/w) GGM solution in mole equivalent of 3:1 NaOH to GGM monomer, and after dissolution, placed in ice bath. DVS in mole equivalent of 1:100 DVS to GGM monomers was added under stirring. After some minutes the solution was transferred to a 45°C water bath where it stood for approximately one hour while being stirred. The expected scheme over the reaction can be seen in Figure 4.

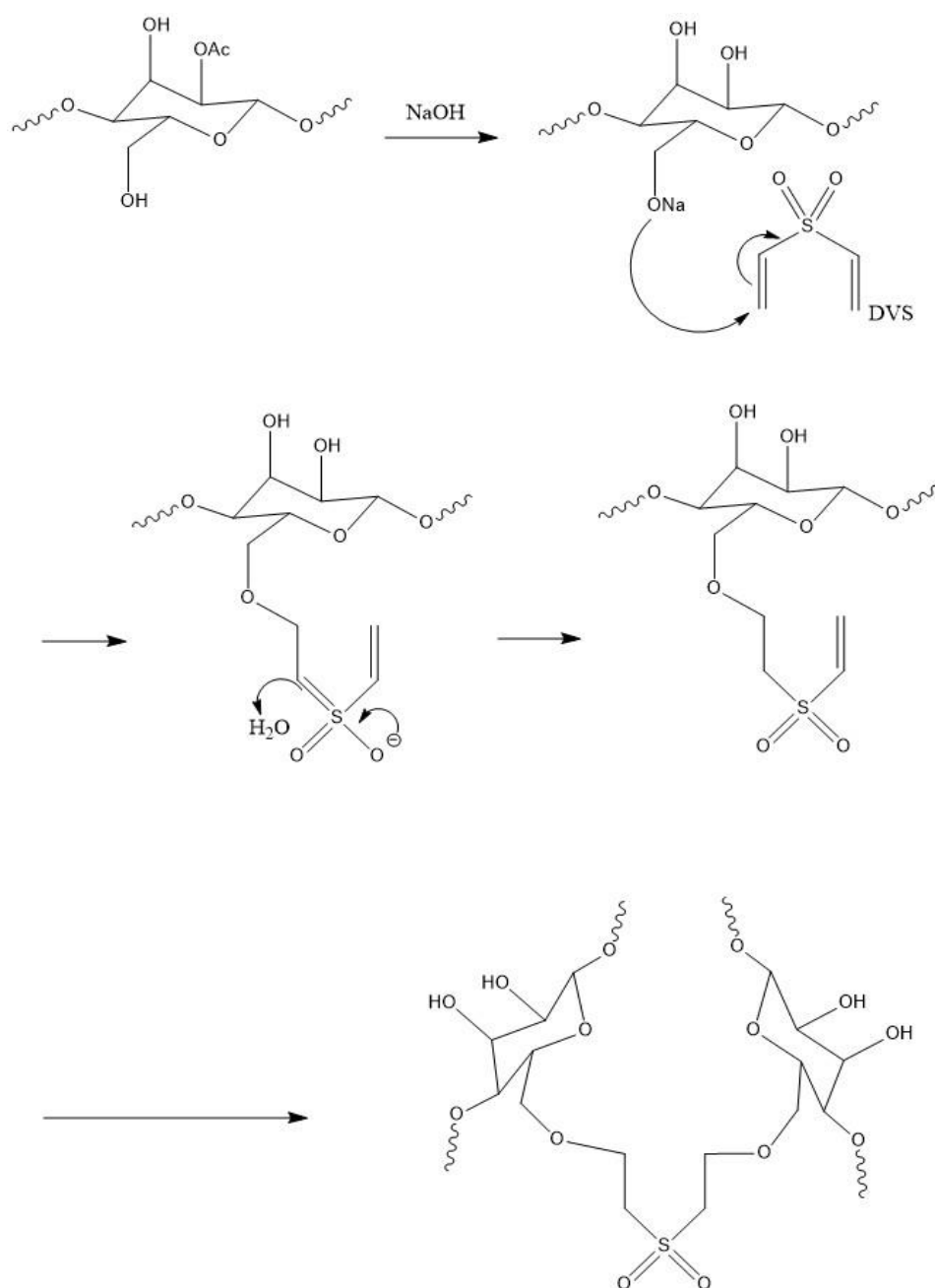


Figure 4. Reaction scheme over the introduction of crosslinks using DVS to the GGM structure, represented by monosaccharide units. The acetyl group (Ac) cleaves with alkali treatment (NaOH).

3.2.3 Introducing hydrophobic side chains to the crosslinked GGM

For protocol over the procedure, see Appendix A.5. NaOH pellets were added to ~260 g GGM-DVS solution (5% (w/w) GGM and 1:100 DVS to GGM monomers) in mole equivalent of 3:1 NaOH to GGM monomer. After dissolution, BGE in mole equivalent of 3:1 BGE to GGM monomer was added and the solution stood overnight in a 45°C oil bath and with stirring at 730 ppm. The solution was then neutralised and a smaller amount dialysed for approximately one week.

3.3 Characterisation analysis

The extracted GGM with different amounts of ethanol was characterised in terms of carbohydrate analysis and molecular weight. The modified GGM was characterised, using pendant drop analysis, thermogravimetric analysis, differential scanning calorimetry, and attenuated total reflection Fourier-transform infrared spectroscopy, and the data was analysed in comparison between themselves and unmodified GGM.

3.3.1 Carbohydrate analysis

For the protocol of the carbohydrate analysis, see Appendix A.6. ~200 mg dried ethanol extracted GGMs were mixed with 3 ml H₂SO₄ (72%), and put under vacuum before transferred to a 30°C shaking water bath for one hour. Afterwards, ~84 g distilled water was added and the samples were put in an 125°C autoclave for one hour. When cooled down, the solutions were filtrated and the filtrates transferred to 100 ml volumetric flask. The solid residues, the Klason lignin, were weighted and the content in the samples calculated.

The diluted filtrates were analysed in respect to their carbohydrate content using a Dionex™ AS-AP Autosampler.

3.3.2 Ultraviolet-visible (UV vis) spectroscopy

The resulting solutions from the preparation before the carbohydrate analysis were analysed with ultraviolet-visible spectroscopy on a Cary 60 instrument scanning wavelength 800 to 200 nm. The absorbance at the wavelength 205 nm was used for calculating the acid soluble lignin concentration in the samples.

3.3.3 Size exclusion chromatography (SEC)

The ethanol extracted GGMs were dissolved in a 0.1 M NaNO₃ and 0.02% NaN₃ solution, and diluted to get a concentration between 0.5-1 mg/ml. The solutions were then filtrated through a 0.45 µm filter and transferred to vials. The SEC analysis was performed on a Wyatt instrument.

3.3.4 Fourier-transform infrared (FTIR) spectroscopy

The ethanol extracted GGMs were milled, mixed with KBr generating 1% (w/w), and pressed into tablets. These tablets were analysed using FTIR spectroscopy with 32 scans, resolution of 4 cm^{-1} at $4000\text{--}400\text{ cm}^{-1}$, and with 2 replicates on a Perkin Elmer Spectrum One instrument.

3.3.5 Pendant drop analysis

The modified GGMs were dissolved in milliQ water generating 1% (w/w) solutions, and from these dilution schemes were produced. The different concentrations were analysed with pendant drop analysis on an Attension Theta optical tensiometer by KSV instruments for getting the surface tension of the samples.

3.3.6 Thermogravimetric analysis (TGA)

The different modified GGMs were dried in room temperature generating films. These together with unmodified GGM in powder form were analysed using a TGA/DSC 3+ Star^e System from Mettler Toledo for TGA that scanned from 30°C up to 550°C .

3.3.7 Differential scanning calorimetry (DSC)

The different modified GGMs were dried in room temperature generating films. These together with unmodified GGM in powder form were analysed using a DSC 2 Star^e System from Mettler Toledo for DSC. The temperature program was initiated with preheating from 25°C to 105°C , then cooling from 105°C to -60°C , heating from -60°C to 200°C , second cooling from 200°C to -60°C , and second heating from -60°C to 250°C . The temperature swipe of interest was the first heating, -60°C to 200°C .

3.3.8 Attenuated total reflection Fourier-transform infrared spectroscopy (ATR-FTIR)

The different modified GGMs were dried in room temperature generating films. These together with unmodified GGM in powder form were analysed using ATR-FTIR with 32 scans, resolution of 4 cm^{-1} at $4000\text{--}400\text{ cm}^{-1}$, and with 2 replicates on a Perkin Elmer Spectrum One instrument.

3.4 Siphon foaming

The siphon experiments were performed using different polymer solutions according to Table 1. The procedure followed the instruction from the manufacture for a commercial siphon. The weight and volume of the generated foam were noted together with pictures direct, 5 minutes, 30 minutes, and then with a time interval of 10 minutes after the foaming.

Table 1. The solutions, including the initial GGM and NFC slurry content, used for the siphon foaming experiments.

Polymer solution	GGM content	NFC slurry content
GGM-NFC	30% (w/w) GGM	10% (w/w) NFC
GGM-NFC	5% (w/w) GGM	11% (w/w) NFC
GGM-BGE	5.91% (w/w) GGM	
GGM-BGE-NFC	5.91% (w/w) GGM	11% (w/w) NFC
GGM-DVS	5% (w/w) GGM	
GGM-DVS	4.28% (w/w) GGM	
GGM-DVS*	4.32% (w/w) GGM	
GGM-DVS-BGE	4.79% (w/w) GGM	
GGM-DVS-BGE-NFC	4.79% (w/w) GGM	10% (w/w) NFC
GGM-DVS-NFC	4.32% (w/w) GGM	11% (w/w) NFC

*Double gas patrons

3.5 Hot-mould baking foam method

To enable optimised usage of material, the hot-mould baking foam method was initiated by investigate if the polymer solution could generate a foam under heat, which was done by analysing a small amount (~1 g) of the samples (~30% (w/w) polymer solution) in a Rheometrics solid analyser RSA11 machine. In the machine the sample solutions were evenly heated in a uniformly distributed heating block. Table 2 shows the different samples and variation in conditions. Before these experiments, unmodified GGM samples had been tested to find a suitable temperature and time. Therefore, the initial temperature for the experiments was 130°C and holding time 10 minutes.

Table 2. The samples and conditions used for the initial step for the hot-mould baking foam method.

	Sample	Conditions
1	GGM-BGE	130°C for 10 minutes
2	GGM-BGE	90°C for 10 minutes
3	GGM-BGE	110°C for 10 minutes
4	GGM-BGE-DVS	110°C for 5 minutes
5	GGM-BGE-DVS	130°C for 5 minutes
6	GGM-DVS	130°C for 5 minutes
7	GGM-BGE-DVS	150°C for 5 minutes
8	GGM-BGE	150°C for 5 minutes
9	GGM-DVS	150°C for 5 minutes
10	GGM-BGE	200°C for 5 minutes
11	GGM-BGE-DVS	200°C for 5 minutes
12	GGM-DVS	200°C for 5 minutes

4.

Results and Discussion

In this chapter the results from the extraction procedure, modification reactions, and the foaming experiments are presented and discussed.

4.1 Characterisation of the extracted GGM

The dry content of the membrane filtrated process water from the manufacturing of TMP is investigated, giving the value 4.67%. This value is used for calculating the yield for the extracted GGMs, which is displayed in Figure 5. Initially the yield is increasing with increasing addition of ethanol, however at a certain point the yield levels out. This maximum level in yield indicates that it is not necessary to have more than double amount of ethanol since the amount precipitate will not increase after that even though the ethanol concentration increases. The total yield of 100% is never reached, which can be since the process water contains other solid residues than GGM, such as salts, and these will not precipitate with addition of ethanol.

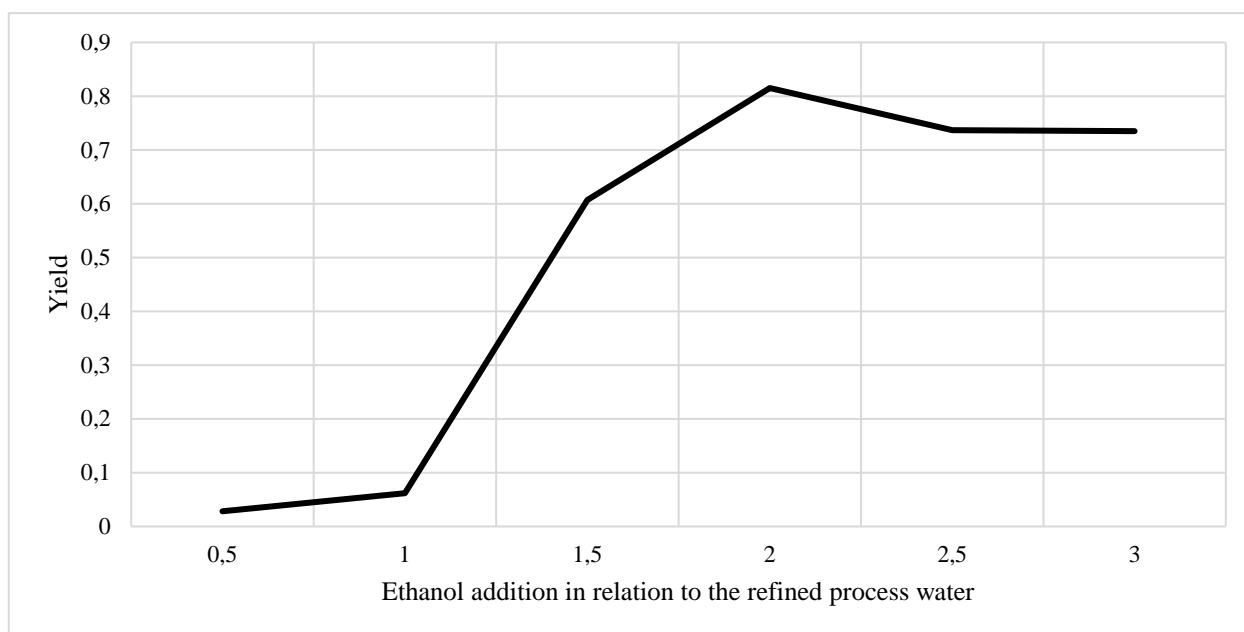


Figure 5. The yield of the precipitations from the ethanol extraction experiments in relation to the concentration of the ethanol.

The result from the carbohydrate analysis is fully displayed in Appendix B.1. The data is an average of the two replicates for each ethanol concentration. The sample with lowest concentration of ethanol had too low amount of precipitate for further analysis. Table 3 shows the galactose, glucose and mannose content of the samples. The GGM sample extracted with one part ethanol to one part process water differs from the other samples and has a higher galactose content. The result indicates that the first residues to precipitate at low addition of ethanol are the ones with higher galactose content, and at higher addition of ethanol the residue with higher mannose content are more eager to precipitate.

The polymers are in water solution, adding ethanol will change the environment to become more hydrophobic. The first to precipitate will be the most hydrophilic, and upon addition of ethanol the hydrophobicity will increase and more hydrophobic parts will precipitate. This means that the GGM with a higher content galactose is less hydrophobic, hence, has higher water solubility which is in line with literature(9). The GGM with more galactose content is more branched, since galactose is in the side chains, and therefore will not be as closely packed as the ones with less branching when in solid state. The higher degree of branching should mean that the polymer is easier to dissolve, than a closely packed structure, and with that rather be in solution. However, in this case, the side chains with galactose making the GGM more hydrophilic can be due to the increase of oxygen in the side chains making the structure more polar.

Table 3. Result from the carbohydrate analysis, showing the ratio of galactose, glucose, and mannose content for the different ethanol extracted GGMs. The data is an average of the two replicates for each ethanol concentration.

Addition Ethanol	Galactose	Glucose	Mannose
1:1	2.28±0.014	1	0.17±0.030
1:1.5	0.88±0.004	1	2.60±0.042
1:2	0.82±0.005	1	2.96±0.007
1:2.5	0.77±0.004	1	2.82±0.042
1:3	0.74±0.000	1	2.77±0.021

The acid soluble lignin and the Klason lignin content are received from the preparation procedure for the carbohydrate analysis of the ethanol extracted GGMs. Table 4 shows the lignin content for the extracted GGMs, as average of the two replicates for each ethanol concentration. For the acid soluble lignin, a general trend displays with decreasing values as the ethanol concentration increases. Higher addition of ethanol will make the acid soluble lignin to rather be soluble in the solution, since the environment will be more hydrophobic. Less alcohol will make the acid soluble lignin to rather be with itself than in the solution and therefore fall out. In contrast, the Klason lignin content, displayed in Table 4, shows values with no general trend, therefore, no conclusion can be drawn. The values for both lignin content are almost the same for all samples, indicating that the lignin content will not be affected by the concentration of ethanol for extraction, which can be due to the overall low lignin content.

Table 4. The acid soluble lignin content and the Klason lignin content in percentage of the total mass of the precipitate for the ethanol extracted GGMs as average of the two replicates for each ethanol concentration.

Addition Ethanol	Acid Soluble Lignin [%]	Klason Lignin [%]
1:1	0.53±0.019	1.25±0.152
1:1.5	0.48±0.013	0.81±0.145
1:2	0.31±0.008	1.12±0.955
1:2.5	0.35±0.028	0.94±0.859
1:3	0.37±0.039	1.25±1.114

The result from the SEC analysis is fully displayed in Appendix B.3. Table 5 shows the number-average molecular weight (Mn), the weight-average molecular weight (Mw), and the polydispersity (Mw/Mn) as average of the two replicates for each ethanol concentration for the extracted GGMs. The Mn displays a general trend in decreasing upon increasing ethanol concentration, meaning that larger molecules precipitate at lower ethanol concentrations. Connecting this result with the result from the carbohydrate analysis, the residue to precipitate at lower ethanol concentration has higher galactose content, hence, more branching and with that are larger molecules. The same behaviour is not seen for the Mw, and consequently not for the polydispersity. The values for the 1:1.5 ethanol addition displays some deviated numbers which are questionable and therefore the analysis of this sample would need to be redone for enabling any conclusions to be drawn.

Table 5. The result from the SEC analysis, the values together with the uncertainty for the number-average molecular weight (M_n), the weight-average molecular weight (M_w), and the polydispersity (M_w/M_n) as average of the two replicates for each ethanol concentration, are displayed for the different ethanol extracted GGMs.

Addition Ethanol	M_n [kDa]	M_w [kDa]	Polydispersity [M_w/M_n]
1:1	29.2± 0.024	39.1± 0.000	1.34± 0.001
1:1.5	21.7± 0.354	69.5± 4.172	3.22± 0.234
1:2	21.3± 11.46	41.3± 37.41	1.72± 0.826
1:2.5	14.0± 0.849	15.5± 0.283	1.11± 0.084
1:3	17.0± 3.677	24.5± 12.66	1.40± 0.447

The result from FTIR analysis for the extracted samples is displayed in Figure 6. The spectra for all samples can be seen in Appendix B.4. The absorption band at $\sim 3400\text{ cm}^{-1}$ corresponds to signals from hydroxyl groups(20) found in for example the carbohydrate units in GGM, or interactions with solvents such as water or ethanol. To separate the bonding signals for each type of hydroxyl group a more careful investigation of this absorption band needs to be performed using for example multivariate analysis. However, changes in this region indicate changes on any of the hydroxyl groups. The absorption band at $\sim 2900\text{ cm}^{-1}$ corresponds to C-H bonding(20), such as CH_2 and CH_3 groups found in the carbohydrate ring structure, the absorption band at $\sim 1750\text{ cm}^{-1}$ corresponds to signals from carbonyl structures(20) which can originate from the acetyl groups found naturally in GGM, and the absorption bands at $\sim 1250\text{ cm}^{-1}$ and $\sim 1100\text{ cm}^{-1}$ correspond to signals related to ether bonding (C-O-C)(20), such as the ether linkages connecting the carbohydrate units in GGM, and in the ring structures.

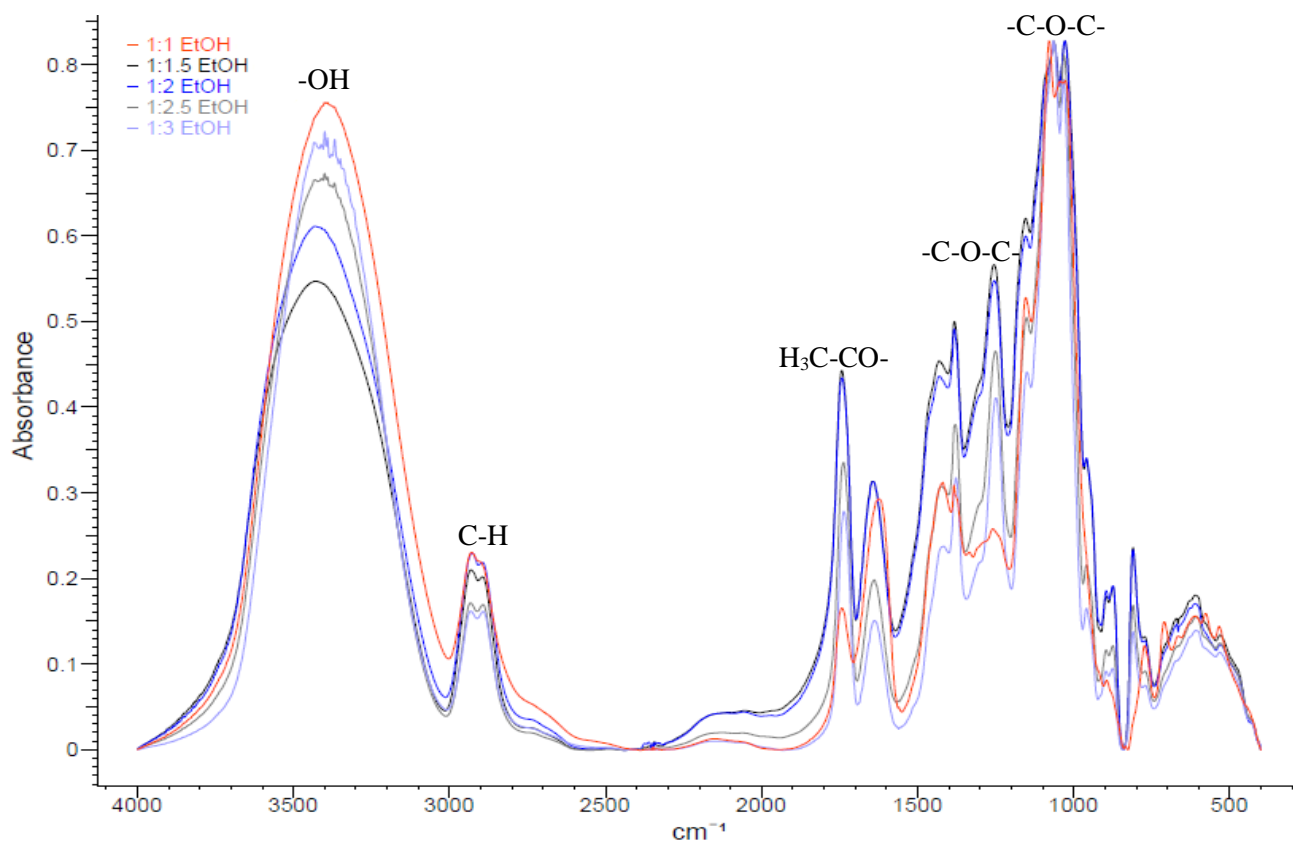


Figure 6. The infrared spectra from the FTIR analysis for the ethanol extracted GGMs.

The ratio from the absorption at $\sim 3400\text{ cm}^{-1}$ and from the ether bonds ($\sim 1250\text{ cm}^{-1}$), see Table 6, are compared for an indication of the acetyl content in the different samples. The more acetyl groups in the sample, fewer interactions with water or ethanol are possible, hence fewer OH interactions. The sample with lowest ethanol concentration displays lowest ratio, indicating highest OH interactions and with that fewer acetyl groups content. This means that higher concentration of ethanol gives precipitation with higher acetyl groups content. The result corresponds to the result from the carbohydrate analysis where a higher mannose content was observed for the sample precipitated at higher ethanol concentrations and the acetyl group are mostly attached to mannose in the GGM structure.

The ratio from the absorption at $\sim 1750\text{ cm}^{-1}$ and from the ether bonds ($\sim 1250\text{ cm}^{-1}$), see Table 6, are compared for an additional indication of the acetyl content in the different samples. Higher ratio would indicate more ether bonds than acetyl groups. The sample with lowest ethanol concentration displays the highest ratio, hence, more ether bonds which corresponds to the comparison for the signals at $\sim 3400\text{ cm}^{-1}$ and the ones from the ether bonds ($\sim 1250\text{ cm}^{-1}$), however, not as distinct.

Table 6. The absorption bands at $\sim 3400\text{ cm}^{-1}$, $\sim 1750\text{ cm}^{-1}$, and $\sim 1250\text{ cm}^{-1}$ from the FTIR for the ethanol extracted GGMs, and the ratio between these absorption bands.

Absorption band				Ratios	
Addition Ethanol	$\sim 3400\text{ cm}^{-1}$	$\sim 1750\text{ cm}^{-1}$	$\sim 1250\text{ cm}^{-1}$	$\sim 1250/\sim 3400$	$\sim 1250/\sim 1750$
1:1	0.76	0.17	0.26	0.34	1.53
1:1.5	0.55	0.45	0.57	1.04	1.27
1:2	0.61	0.45	0.54	0.89	1.20
1:2.5	0.66	0.34	0.46	0.70	1.35
1:3	0.71	0.28	0.41	0.58	1.46

The choice of extraction procedure for further modification of extracted GGM was grounded on the ethanol concentration giving the highest yield together with the most common ratio of carbohydrate units found in nature, resulting in the procedure where double amount of ethanol in relation to process water was used.

4.2 Analysis of the modifications of GGM

Figure 7 displays the result from the surface tension measurements and as can be seen the samples modified with BGE (GGM-BGE and GGM-DVS-BGE) reduce the surface tension significant in comparison to the unmodified GGM and GGM-DVS. This means that GGM-BGE and GGM-DVS-BGE are more surface active and the decreased surface tension can be an indication that the modifications with BGE were successful.

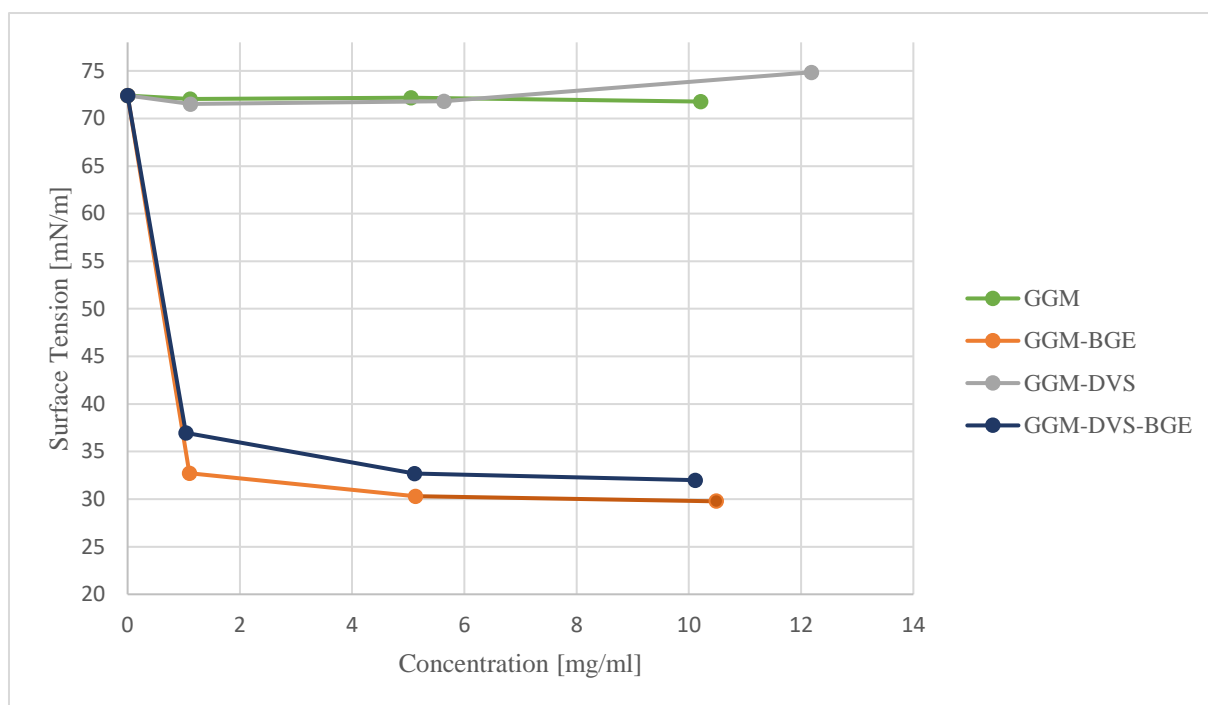


Figure 7. The surface tension results from the pendent drop analysis for the modified GGMs and an unmodified as reference.

The result from the TGA analysis for the modified GGM samples and an unmodified GGM sample as reference is presented in Figure 8. In the beginning of the graphs near 100°C, the water loss of the samples is displayed and as can be seen, the unmodified GGM has a sharper decreasing slope than the other samples, hence, has higher water loss. This means that the

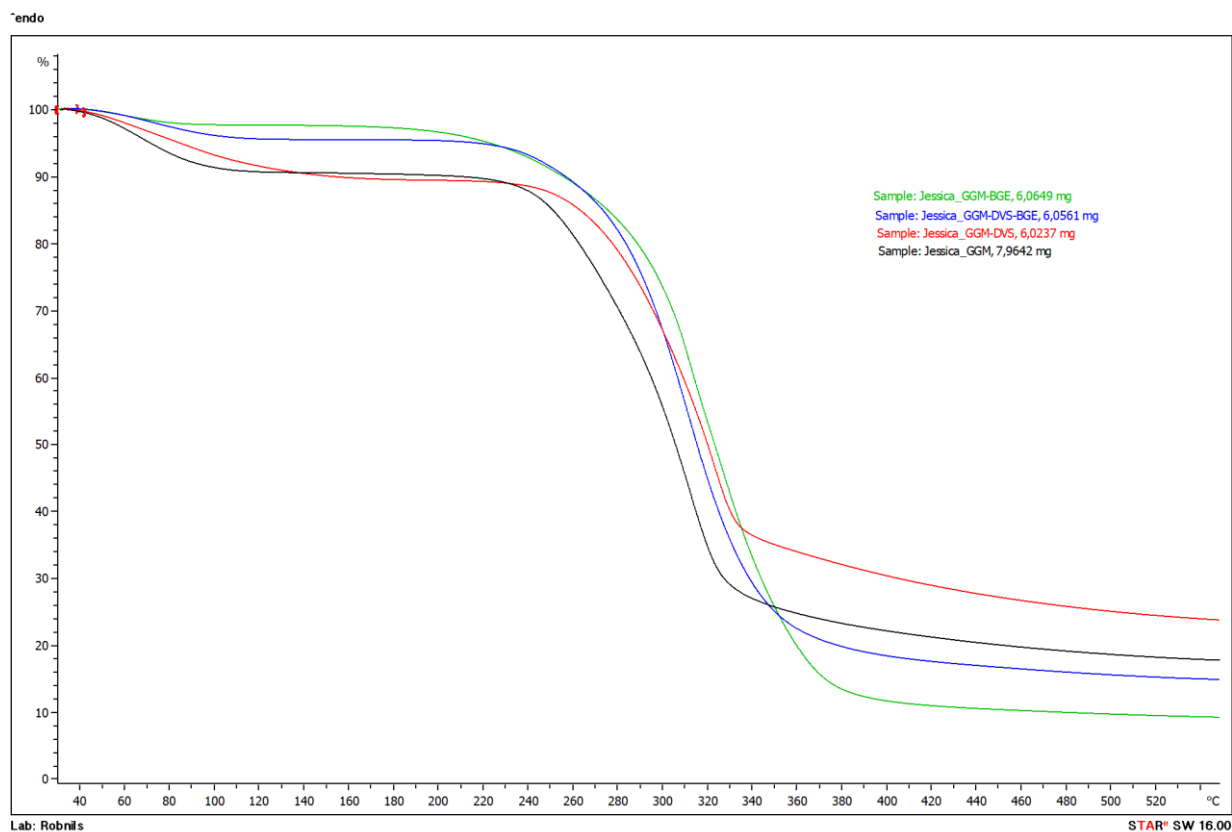


Figure 8. The result from TGA analysis for the modified GGMs and an unmodified as reference.

unmodified GGM sample consist of more water. The samples modified with BGE (GGM-BGE and GGM-DVS-BGE) display lower water loss, implying that these samples consist of less water and are more hydrophobic which indicate successful modifications with BGE.

The GGM-DVS sample displays a higher temperature before the degradation occurs, in comparison with the other samples, which can be explained by the crosslinks in the sample. During the crosslinking reaction for increasing the molecular weight by connecting GGM molecules, new bonds are formed and with that more energy (higher temperature) is required to degrade the sample. This may be a reason for the displayed higher degradation temperature. Also, the GGM-DVS displays a decreasing slope around 100°C that is sharper than the BGE modified samples, indicating that GGM-DVS would contain more water than these samples since the water loss is higher.

The result from DSC analysis is displayed in Figure 9, with heating from -60°C to 200°C, where the peaks are expected to be due to water evaporation, and can therefore be a measurement of the water fraction in the samples. The energy representing each peak can be used for calculating the water loss, see Appendix B.5. The peaks are expected to be from the water loss when sample is heated, and by using the heat of vaporisation for water the amount of water loss can be calculated, and since the sample weight is known the water fraction for each sample can be assumed. From these calculations, the water fractions are 1.02% for GGM-BGE, 1.27% for GGM-DVS-BGE, 4.29% for GGM-DVS, and 4.71% for unmodified GGM. The samples modified with BGE (GGM-BGE and GGM-DVS-BGE) have lower water fraction, meaning that the unmodified GGM and GGM modified with DVS bind more water. This goes in line with the results from the TGA analysis.

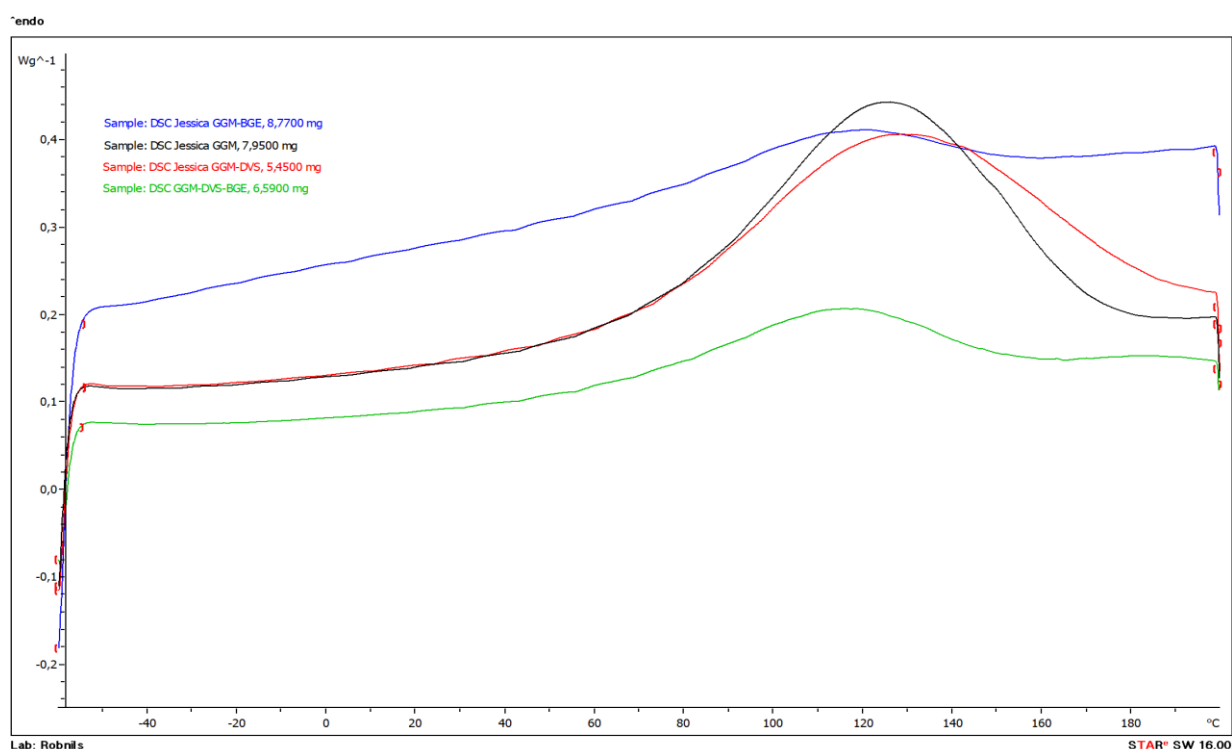


Figure 9. The result from DSC analysis, heating range -60°C to 200°C, for the modified GGMs and an unmodified as reference. The peaks correspond to water evaporation.

The result from ATR-FTIR for the modified GGM samples and an unmodified GGM sample as reference can be displayed in Figure 10. The unmodified sample has an absorption band at $\sim 1750\text{ cm}^{-1}$ corresponding to signals from naturally occurring acetyl groups(20) in GGM and is not displayed for the other modified samples. The modified samples have been exposed to sodium hydroxide, which are known to cleave the acetyl groups from GGM.

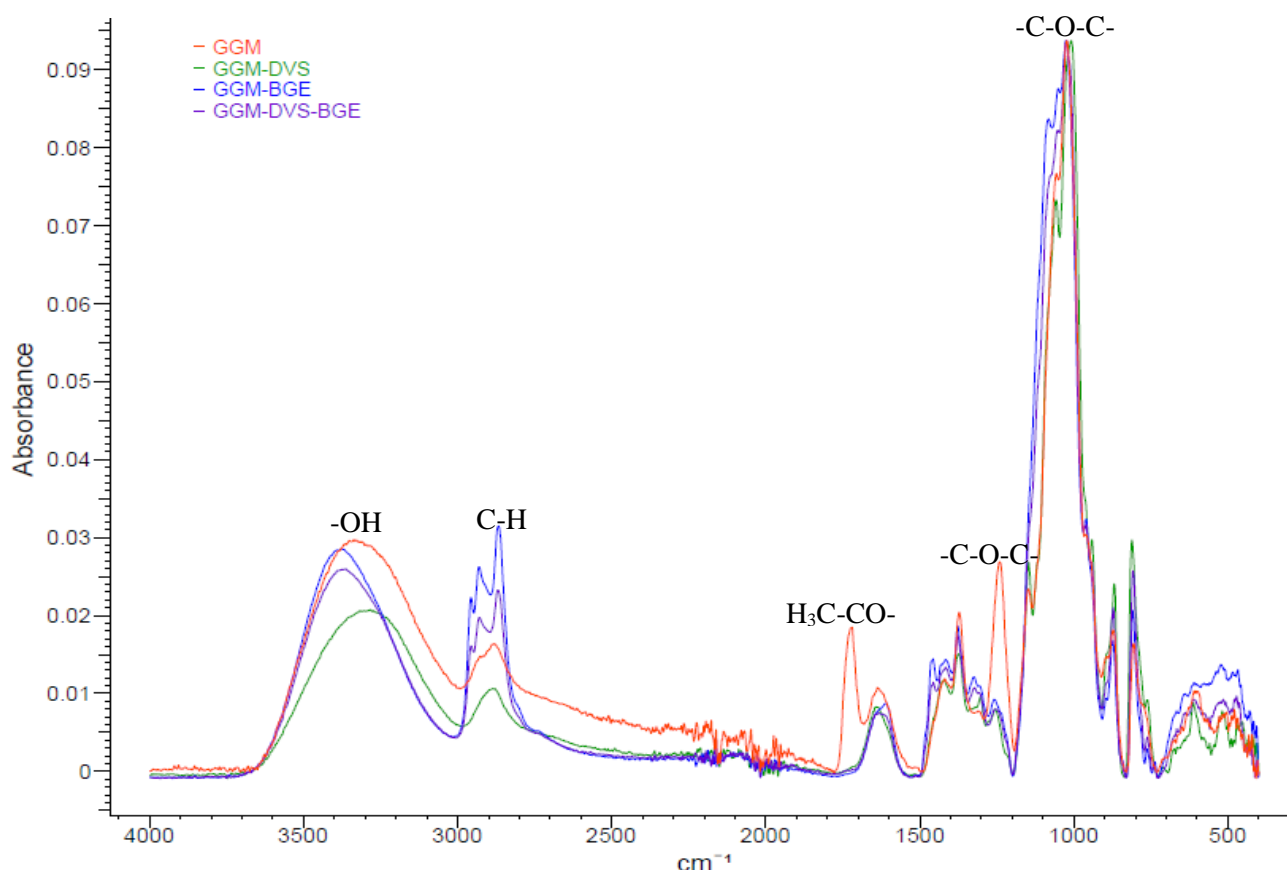


Figure 10. The ATR-FTIR spectra for the modified GGMs and an unmodified as reference.

The absorption bands expected to be from C-H ($\sim 2900\text{ cm}^{-1}$) are compared to the ones expected to be from ether linkage ($\sim 1250\text{ cm}^{-1}$)(20), see Table 7. From the comparison of these signals, the samples modified with BGE (GGM-BGE and GGM-DVS-BGE) have a lower ratio and with that higher signals from C-H. This indicates that these samples have more CH_2 and CH_3 carbons, meaning that the modifications with BGE have been successful. Another indication for a change in the molecular structure for the BGE-modified samples is the shift of the absorption band at $\sim 3400\text{ cm}^{-1}$, corresponding to the hydroxyl groups(20). The signal has been shifted to higher wavenumbers indicating changes in the amount of hydroxyl groups or number of interactions with the hydroxyl groups.

Table 7. The absorption bands at $\sim 2900\text{ cm}^{-1}$, and $\sim 1250\text{ cm}^{-1}$ from the ATR-FTIR for the modified GGMs with an unmodified as reference, and the ratio between these absorption bands.

Sample	Absorption bands		Ratio
	$\sim 2900\text{ cm}^{-1}$	$\sim 1250\text{ cm}^{-1}$	$\sim 1250/\sim 2900$
GGM	0.160	0.027	1.690
GGM-DVS	0.011	0.009	0.818
GGM-BGE	0.031	0.011	0.355
GGM-DVS-BGE	0.023	0.008	0.348

For the modification with DVS, the samples should contain a sulfone group linking the carbon chains together. The spectra from GGM-DVS sample displays a small absorption band at $\sim 1300\text{ cm}^{-1}$ which correspond to sulfone group(20), indicating that the sample contains sulfone. However, the sample modified with both DVS and BGE do not display this signal. This could indicate the sulfone groups have been cleaved during the modification with BGE or that the signal is small and with that hard to distinguish.

In addition, comparing the spectrum from the unmodified ethanol extracted GGM in ATR-FTIR with the spectra for the ethanol extracted ones in FTIR, Figure 10 and Figure 6, shows some variation in intensity. This can be due to the differences in the methods, where in ATR the IR light reflects from a crystal and detect the sample surface. In FTIR using KBr tablets, the IR light is absorbed by the bulk of the sample.

The results for the GGM-DVS sample, from TGA and DSC, show, in general, the same trends as for the unmodified GGM in respect of water content. Modifying the GGM with the crosslinking agent DVS for the generation of higher molecular weight, the concentration of DVS is kept low for not generating too many attachment points between the chains which is not desirable due to that a highly crosslinked gel will hinder the formation of a cellular structure. This leading to that only a few of all possible reactive sites on the GGM molecule will be occupied, meaning that the interaction with water will not be as affected as for the modifications with BGE.

From the optimising crosslinking reaction, the first agent to be tested was ethylene glycol diglycidyl ether (EGDE) since it has two epoxy sites at each end and that is thought to be favourable in the generation of longer molecular chains. However, the agent, even at high excess, did not performed as good and no visible thickness could be notice. Increasing the chain length is expected to increase the viscosity and generate a thicker solution. The other agent, DVS, was chosen as candidate due to the proven effect with other polymers such as hyaluronic acid(27)(28). The usage of crosslinking agents for the generation of longer chains and increased molecular weight is depended on the viscosity of the sample. This optimising procedure can therefore, be improved by rheology measurements and a further investigation of the viscosity.

4.3 Results from the siphon foaming experiments

In the siphon foaming experiments all samples except GGM-DVS generated a foam structure. The results for all the different samples are displayed in Appendix B.6. The volume of the foam in relation to the total volume, including the foam and liquid, for different time scales and samples is displayed in Figure 11. The comparison between the foams generated from unmodified GGM and the BGE modified ones clearly demonstrate an increase in foam ratio over time for the BGE modified samples. Figure 12 illustrates the foam volume of the samples for different time scales in relation to the initial foam volume. This can be an indicator for the stability of the generated foams. The same trends can be observed here as in Figure 11, the GGM samples modified with BGE show lower reduction in foam volume over time in comparison with the unmodified GGM, hence, are more stable.

From the surface tension experiments, GGM-BGE and GGM-DVS-BGE show increased surface activity in comparison with unmodified GGM and GGM modified with DVS, see Figure 7, which is a result in line with the ones from the siphon tests. The increase in hydrophobicity will make the polymer more amphiphilic and enable arrangement at the interface, lower the surface tension and helping prevent rapture of the bubble. Therefore, the modification with BGE for increasing the hydrophobicity and give higher surface activity is expected to generate a more stable foam. Addition of NFC increases the stability of the foam further which is clearly displayed in Figure 11 and Figure 12, and goes in line with the expectation that the NFC may assembly at the interface of the bubbles and increase the viscosity of the sample.

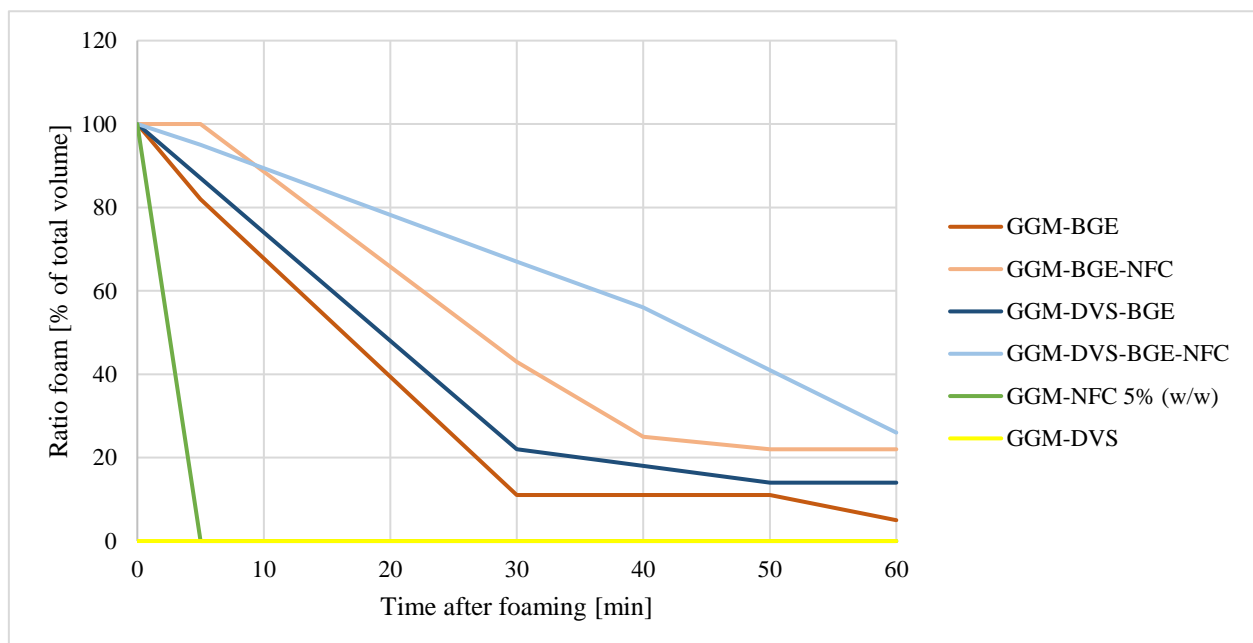


Figure 11. Result from the siphon foaming experiments showing the percentage of foam in relation to the total sample volume as function of time after the foaming procedure. GGM-DVS represents all the foaming experiments with the DVS modified GGM, even the one mixed with NFC, since none of them generated a foam. The sample for GGM (30% (w/w)) is not represented, since it did not generate a foam.

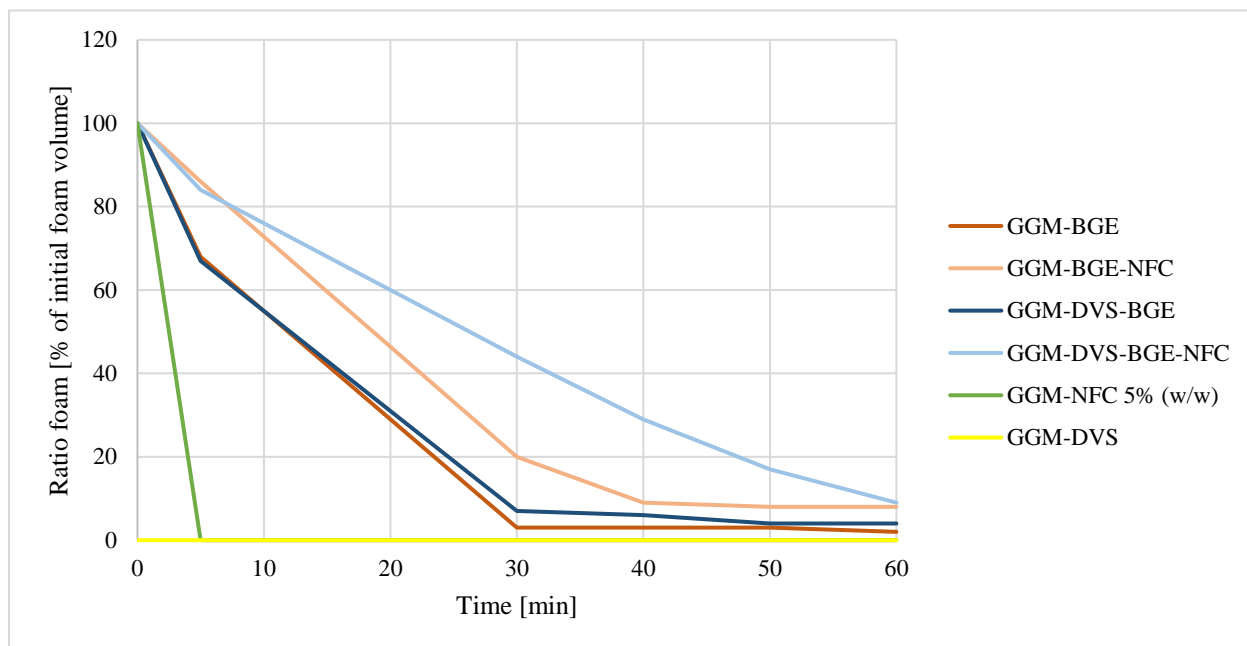


Figure 12. Result from the siphon foaming experiments showing the percentage of foam in relation to initial foam volume as function of time after the foaming procedure. GGM-DVS represents all the foaming experiments with the DVS modified GGM, even the one mixed with NFC, since none of them generated a foam. The sample for GGM (30% (w/w)) is not represented, since it did not generate a foam.

There are different factors affecting the foamability of the samples, including the viscosity. The usage of 30% (w/w) GGM solution, see Appendix B.6, did not generate a foam. If the sample has too high viscosity, the nitrous oxide gas used in the siphon will not be able to mix with the solution and, hence, not generate a cellular structure. However, the polymer solution should not have too low viscosity either since the gas bubbles can move and coalesce, which is a result of that the solution is not able to keep the cellular structure. If the viscosity is too low, the bubbles will not be kept and on the contrary, if the viscosity is too high the bubbles will not be formed.

Since the unmodified sample and the BGE modified samples generated foams initially, the problem is the stability. If the generated foam had, for example, been freeze dried directly, the foam would probably be more stable. The generated foam has fast degradation, making it unstable and the cellular structure fall apart in a short time range.

4.4 Result from the initial step for the hot-mould baking foam method

The results from the initial step for the hot-mould baking foam method were unsatisfying, where no sample generated a foam or cellular structure. Figure 13 shows some of the failed experiments, where no cellular structure can be displayed. The GGM-DVS is still wet, and

both GGM-BGE and GGM-DVS-BGE samples are sticky. Therefore, the hot-mould baking foam method was never investigated.



Figure 13. Results from the initial step for the hot-mould baking foam method, temperature of 150°C and holding time of 5 minutes. Left to right, GGM-DVS, GGM-BGE, GGM-DVS-BGE.

5.

Conclusion and Future Outlook

The GGM is proven to generate a cellular structure, hence creating a foam. However, the generated foam has some stability limitations.

The modification of GGM with the purpose to increase the hydrophobic nature by introducing longer side chains, using BGE, would generate an amphiphilic character which was confirmed by the surface tension measurements. This increased the stability of the generated foam, in comparison with the unmodified sample. The addition of NFC increased the stability further. The modification of GGM with the purpose to increase the molecular weight by introducing crosslinking between the GGM chains, using DVS, did not generate a foam and did not show any tendency to have an increase in surface activity. The outcome of this project therefore indicates that the best candidates for the foaming are the GGM modified with BGE (GGM-BGE and GGM-DVS-BGE) and mixed with NFC, which gave the most stable foam using the siphon foaming method.

For the extraction procedure, the results indicate that no more than a ratio of 1:2 ethanol addition is required for a high yield. Additionally, the extracted GGMs exhibit variation in the carbohydrate content, molecular weight, and functional group. Higher concentration of ethanol generated GGM with higher mannose content, and more acetyl groups, and a higher number-average molecular weight. To further optimise the extraction procedure, the differences between the samples extracted with different ethanol concentrations need some supplementary characterisations, for example by nuclear magnetic resonance spectroscopy. The analysis in respect of molecular weight gave in this project some faulty values and therefore need further analysis for any conclusions.

The result from this project indicate that GGM can create a foam, however the stability of the foam is in a time range of under 60 minutes. For future investigation the challenges lie within the field of foam stability and how to conserve the generated foam. Besides, further investigation needs for enable foaming of GGM using hot-mould baking methods. This includes deeper analysis of the thermal behaviour of the GGM molecule, preferable with the modification for increased hydrophobicity.

References

1. Bajpai P. Pulp and paper industry: chemicals. Amsterdam;Boston; Elsevier; 2015.
2. Sjöström E, Alén R, editors. Analytic Methods in Wood Chemistry, Pulping, and Papersmaking. 1st ed. New york: Springer-Verlag Berlin Heidelberg; 1999.
3. Karlsson K, Kádár R, Stading M, Rigdahl M, RISE. Processing window for extrusion foaming of hydroxypropyl methylcellulose. Vol. 23, Cellulose. Dordrecht: Springer Netherlands; 2016. p. 1675–85.
4. Eaves D. Handbook of polymer foams. Shawbury, Shrewsbury, Shropshire, U.K: Rapra Technology; 2004.
5. Song T. Extraction of polymeric galactoglucomannans from spruce wood by pressurised hot wate. Åbo Akademi University; 2013.
6. Iannace S, Park CB, editors. Biofoams: science and applications of bio-based cellular and porous materials. In: Biofoams: science and applications of bio-based cellular and porous materials. CRC Press; 2016.
7. Bajpai P. Green Chemistry and Sustainability in Pulp and Paper Industry. 2015th ed. Cham: Springer International Publishing; 2015.
8. Mekanisk pappersmassa. In: Nationalencyklopedin [Internet]. Available from: <http://www.ne.se/uppslagsverk/encyklopedi/lång/mechanisk-pappersmassa>
9. Ek M, Gellerstedt G, Henriksson G. Wood Chemistry and Wood Biotechnology. Vol. 1. Berlin ;Boston: De Gruyter; 2009.

10. Gymnosperm. In: Nationalencyklopedin [Internet]. Available from: <http://www.ne.se/uppslagsverk/ordbok/svensk/gymnosperm>
11. Angiosperm. In: Nationalencyklopedin [Internet]. Available from: <http://www.ne.se/uppslagsverk/ordbok/svensk/angiosperm>
12. Abe A, Dušek K, Kobayashi S, Błażewicz S. Biopolymers: lignin, proteins, bioactive nanocomposites. Vol. 232;232.; Berlin: Springer; 2010.
13. Ebringerová A. Structural diversity and application potential of hemicelluloses. Vol. 232, Macromolecular symposia. Wiley Online Library; 2005. p. 1–12.
14. Song T, Pranovich A, Sumerskiy I, Holmbom B. Extraction of galactoglucomannan from spruce wood with pressurised hot water. Vol. 62, *Holzforschung*. Berlin: Walter De Gruyter & co; 2008. p. 659–66.
15. Capek P, Kubačková M, Alföldi J, Bilisics L, Lišková D, Kákoniová D. Galactoglucomannan from the secondary cell wall of *Picea abies* L. Karst. Vol. 329, *Carbohydrate Research*. Oxford: Elsevier Ltd; 2000. p. 635–45.
16. Thuvander J, Jönsson AS. Extraction of galactoglucomannan from thermomechanical pulp mill process water by microfiltration and ultrafiltration-Influence of microfiltration membrane pore size on ultrafiltration performance. Vol. 105, *Chemical Engineering Research & Design*. 2016. p. 171–6.
17. Cervin NT, Andersson L, Ng JBS, Olin P, Bergström L, Waišgberg L, et al. Lightweight and strong cellulose materials made from aqueous foams stabilized by nanofibrillated cellulose. Vol. 14, *Biomacromolecules*. Washington: American Chemical Society; 2013. p. 503–11.
18. Troglér WC. Physical properties and mechanisms of formation of nitrous oxide. Vol. 187, *Coordination Chemistry Reviews*. Lausanne: Elsevier B.V; 1999. p. 303–27.
19. Karlsson K, Schuster E, Stading M, Rigdahl M, Institutionen för material- och tillverkningsteknik P material och kompositer, Department of Materials and Manufacturing Technology PM and C. Foaming behavior of water-soluble cellulose derivatives: hydroxypropyl methylcellulose and ethyl hydroxyethyl cellulose. Vol. 22, *Cellulose*. Dordrecht: Springer Netherlands; 2015. p. 2651–64.
20. Pavia DL. Introduction to spectroscopy. 4th ed. Belmont, CA;Australia; Brooks/Cole Cengage Learning; 2009.
21. Song T, Pranovich A, Holmbom B. Characterisation of Norway spruce hemicelluloses extracted by pressurised hot-water extraction (ASE) in the presence of sodium bicarbonate. Vol. 65, *Holzforschung*. Berlin: Walter De Gruyter GmbH; 2011. p. 35–42.
22. Willför S, Sjöholm R, Laine C, Roslund M, Hemming J, Holmbom B. Characterisation of water-soluble galactoglucomannans from Norway spruce wood and thermomechanical pulp. Vol. 52, *Carbohydrate Polymers*. Oxford: Elsevier Ltd; 2003. p. 175–87.
23. Nypelö T, Laine C, Aoki M, Tammelin T, Henniges U. Etherification of Wood-Based Hemicelluloses for Interfacial Activity. Vol. 17, *Biomacromolecules*. United States; 2016. p. 1894–901.

24. Melnick RL. Carcinogenicity and Mechanistic Insights on the Behavior of Epoxides and Epoxide-Forming Chemicals. Vol. 982, *Annals of the New York Academy of Sciences*. Blackwell Publishing Ltd; 2006. p. 177–89.
25. Oyama T. Cross-Linked Polymer Synthesis BT - *Encyclopedia of Polymeric Nanomaterials*. In: Kobayashi S, Müllen K, editors. *Encyclopedia of Polymeric Nanomaterials*. Berlin, Heidelberg: Springer Berlin Heidelberg; 2014. p. 1–11.
26. Peresin MS, Kammiovirta K, Setälä H, Tammelin T. Structural Features and Water Interactions of Etherified Xylan Thin Films. Vol. 20, *Journal of Polymers and the Environment*. Boston: Springer US; 2012. p. 895–904.
27. Sannino A, Madaghiele M, Conversano F, Mele G, Maffezzoli A, Netti PA, et al. Cellulose derivative-hyaluronic acid-based microporous hydrogels cross-linked through divinyl sulfone (DVS) to modulate equilibrium sorption capacity and network stability. Vol. 5, *Biomacromolecules*. Washington: American Chemical Society; 2004. p. 92–6.
28. Mondal S, Haridas N, Letha SS, Vijith V, Rajmohan G, Rosemary MJ. Development of injectable high molecular weight hyaluronic acid hydrogels for cartilage regeneration. Vol. 53, *Journal of Macromolecular Science, Part A*. Philadelphia: Taylor & Francis; 2016. p. 507–14.

Appendix

Appendix A - Protocols

A.1 Extraction procedure

The different amount of ethanol (95%) and refined process water used for the extraction experiments shown in Table A. 1.

Table A. 1. Different amount of ethanol (95%) and refined process water generating different ratios for the extraction procedure.

Ratios	Refined process water [g]	95% Ethanol [g]
1:0.5	101.23	53.28
1:0.5	103.83	51.40
1:1.5	102.47	151.11
1:1.5	106.24	152.20
1:2	100.46	200.09
1:2	100.49	200.20
1:2.5	101.90	250.18
1:2.5	101.47	250.09

1:3	100.21	300.80
1:3	100.23	300.58
1:1	100.70	100.77
1:1	100.53	100.52

A.2 Crosslinking procedure optimisation

Ethanol extracted GGM was dissolved in milliQ water, in which NaOH pellets were added in mole equivalent of 3:1 NaOH to GGM monomer. After total dissolution, the solution was put on ice and stirring. The crosslinker was then added and after approximately 3 minutes placed on ice, the solution was transferred to water bath (45°C) for approximately one hour.

The same procedure was performed with different weight-to-weight ratios of GGM solutions and with variation in ratio of the crosslinking agent and with different crosslinking agent, see Table A. 2

Table A. 2. The GGM solutions, crosslinking agents, and ratio of GGM to crosslinking, that were varied for the crosslinking procedure optimisation.

GGM solution [w/w]	Crosslinking agent	Ratio of GGM to crosslinking agent
6.86%	EGDE ^a	2:7
6.86%	EGDE	1:7
6.86%	EGDE	1:14
7.00%	EGDE	1:1
4.00%	EGDE	12:1
4.00%	EGDE	1:4
4.00%	EGDE	1:8
4.00%	EGDE	1:2
10.0%	EGDE	1:5
10.0%	DVS ^b	1:10
10.0%	DVS	1:40
10.0%	DVS	1:100

^aEthylene glycol diglycidyl ether, ^bDivinyl sulfone

A.3 Protocol for introducing hydrophobic side chains to the GGM

200.04 g 10% (w/w) GGM solution was transferred to a three-necked round flask with septum for nitrogen gas and with a cooler, and was put in an oil bath (45°C) and 730 ppm stirring. 14.7 g NaOH pellets in mole equivalent of 3:1 NaOH to GGM monomer was added and the solution stood for one hour for complete dissolution of the pellets. Afterwards, 53 ml BGE (mole equivalent of 3:1 BGE to GGM monomer) was added dropwise under 50 minutes and

then the solution stood overnight in the oil bath while being stirred. Thereafter, the solution got cooled down before it was neutralised with H_2SO_4 and NaOH, and transferred to dialysis membrane. The solution was on dialysis for approximately one week.

A.4 Protocol for introducing crosslinks to GGM for increasing the molecular weight

38.33 g ethanol extracted GGM was dissolved in 700.3 g milliQ water, generating a 5% (w/w) solution. In the solution there were some small black particles, which were removed by centrifugation. To 600 g of the solution, 22.11 g NaOH pellets were added in mole equivalent of 3:1 NaOH to GGM monomer. The pH value was analysed.

622 g of 5% (w/w) GGM-NaOH-solution, was put on ice and stirring, and 265 μl DVS was added in mole equivalent of 1:100 DVS to GGM monomers. The solution stood approximately for 3 minutes on ice and then the solution was transferred to water bath (45°C) and stood for stirring approximately one hour. Afterwards, the solution was neutralised with H_2SO_4 and NaOH. Stood in room temperature overnight. The next day, a small amount of the solution (13.3 g) was transferred to a dialysis membrane for further analysis.

A.5 Protocol for introducing hydrophobic side chains to the crosslinked GGM

258.81 g DVS-GGM solution (5% (w/w) GGM and 1:100 DVS to GGM monomers) was transferred to a three-necked round flask with septum for nitrogen gas and with a cooler, and was put in an oil bath (45°C) and 730 ppm stirring. 9.59 g NaOH pellets in mole equivalent of 3:1 NaOH to GGM monomer was added and the solution stood for approximately one hour for complete dissolution of the pellets. Afterwards, 34 ml of BGE (mole equivalent of 3:1 BGE to GGM monomer) was added dropwise under 20 minutes and then the solution stood overnight in the oil bath while being stirred. Thereafter, the solution got cooled down before it was neutralised with H_2SO_4 and NaOH, and transferred to dialysis membrane. The solution was on dialysis for approximately one week.

A.6 Protocol for the carbohydrate analysis

The ethanol extracted GGMs were dried overnight in oven (70°C). ~200 mg was transferred to beakers and 3 ml H_2SO_4 (72%) was added, and the beakers were put under vacuum in an exicator for 15 minutes. Then the beakers were transferred to a shaking water bath (30°C) for one hour. Afterwards, ~84 g distilled water was added and the beakers were covered with alumina covers and put in an autoclave (125°C) for one hour. When the beakers cooled down the solutions were filtrated and the filtrate transferred to 100 ml volumetric flask. The solid residues, the Klason lignin, were weighted and the content in the samples calculated. The

diluted filtrates were analysed in respect to their carbohydrate content using a Dionex™ AS-AP Autosampler.

Appendix B – Results

B.1 Result from the carbohydrate analysis for the ethanol extracted GGM

The result from the carbohydrate analysis is displayed in Table B. 1.

Table B. 1. The result from the carbohydrate analysis, which shows the monosaccharides content of the different ethanol extracted GGMs.

Addition Ethanol	Arabinose	Rhamnose	Galactose	Glucose	Xylose	Mannose
1:1	0.22±0.005	0.01±0.001	2.28±0.014	1	0.012±0.003	0.17±0.030
1:1.5	0.09±0.0001	0.005±9.8E-5	0.88±0.004	1	0.011±1.4E-4	2.60±0.042
1:2	0.09±0.001	0.0061±4.5E-5	0.82±0.005	1	0.012±2.8E-5	2.96±0.007
1:2.5	0.08±0.001	0.0049±7.7E-4	0.77±0.004	1	0.012±1.6E-4	2.82±0.042
1:3	0.08±0.001	0.0039±5.9E-4	0.74±0.000	1	0.012±9.9E-5	2.77±0.021

B.2 Lignin content for the ethanol extracted GGM

The acid soluble lignin and the Klason lignin content were received from the preparation procedure for the carbohydrate analysis of the ethanol extracted GGMs. Table B. 2 displays the results for the lignin content for the extracted GGMs.

Table B. 2. The acid soluble lignin content and the Klason lignin content in percentage of the total mass of the precipitate for the ethanol extracted GGMs.

Addition Ethanol	Acid Soluble Lignin [%]	Klason Lignin [%]
1:1	0.53±0.019	1.25±0.152
1:1.5	0.48±0.013	0.81±0.145
1:2	0.31±0.008	1.12±0.955
1:2.5	0.35±0.028	0.94±0.859
1:3	0.37±0.039	1.25±1.114

B.3 Result from the SEC analysis of the ethanol extracted GGM

The results from SEC analysis for the ethanol extracted GGMs are displayed in Table B. 3.

Table B. 3. The result from the SEC analysis for the ethanol extracted GGMs. Showing the number-average molecular weight (M_n), the weight-average molecular weight (M_w), and the polydispersity (M_w/M_n), the uncertainty weighted radius average (r (avg)), the hydrodynamic radius ($rh(v)$), the injected mass, the calculated mass, the mass fraction, the mass recovery, the peak range, and the weight-average intrinsic viscosity ($[\eta]_w$). The results are averaged of the two replicates for each ethanol concentration.

	Mn [kDa]	Mw [kDa]	Polydispersity [Mw/Mn]	r(avg) [nm]	rh(v)(avg) [nm]	Injected mass [μg]	Calculated mass [μg]	Mass fraction [%]	Mass recovery [%]	Peak range [min]	$[\eta]_w$ [mL/g]
1:1	29.2± 0.024	39.1± 0.000	1.34± 0.0007	13.1±1.44	4.22±0.024	70.0±0.00	73.7±1.24	100.0	105.2±1.77	13.2-18.3	15.9±0.242
1:1.5	21.7± 0.354	69.5± 4.17	3.22± 0.234	28.9±0.141	6.15±0.071	75.5±4.45	101.9±11.1	100.0	134.8±6.79	10.4-18.6	65.5±1.548
1:2	21.3± 11.5	41.3± 37.4	1.72± 0.826	18.3±7.43	5.75±0.212	68.0±2.90	87.1±1.39	100.0	128.4±7.57	11.1-19.0	61.5±0.276
1:2.5	14.0± 0.849	15.5± 0.283	1.11± 0.084	15.7±5.23	5.45±0.071	70.0±0.00	115.2±15.1	100.0	164.5±21.5	10.9-18.9	60.8±0.123
1:3	17.0± 3.68	24.5± 12.7	1.40± 0.447	17.0±9.12	5.45±0.071	70.0±0.00	113.7±4.03	100.0	162.4±5.73	11.1-19.4	59.8±1.167

B.4 FTIR result for the ethanol extracted GGM

The result from the FTIR analysis of the ethanol extracted GGMs can be displayed in Figure B.1-B.5, where each figure represents one ethanol ratio.

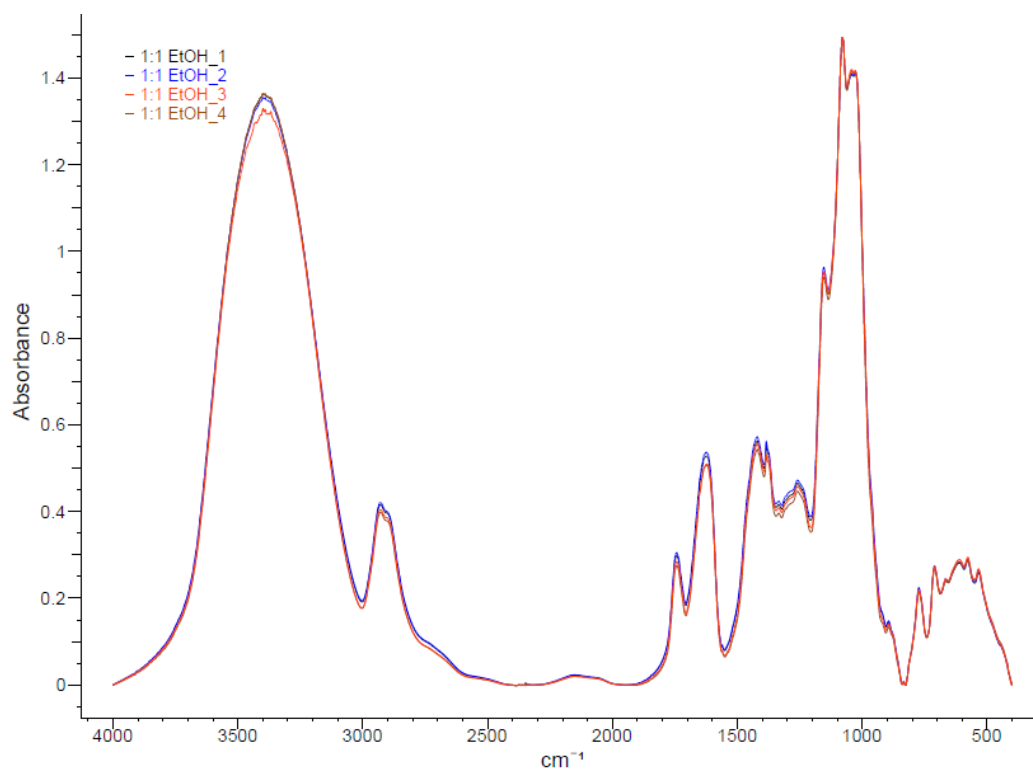


Figure B. 1. FTIR spectra for the 1:1 ethanol extracted GGM samples.

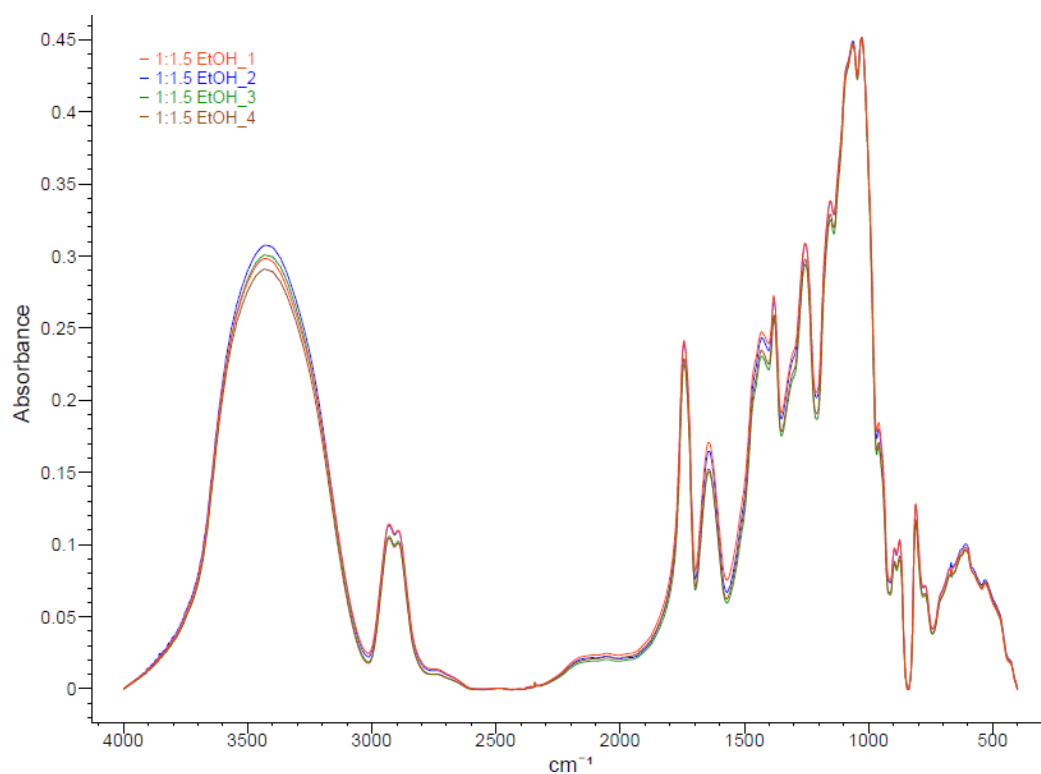


Figure B. 2. FTIR spectra for the 1:1.5 ethanol extracted GGM samples.

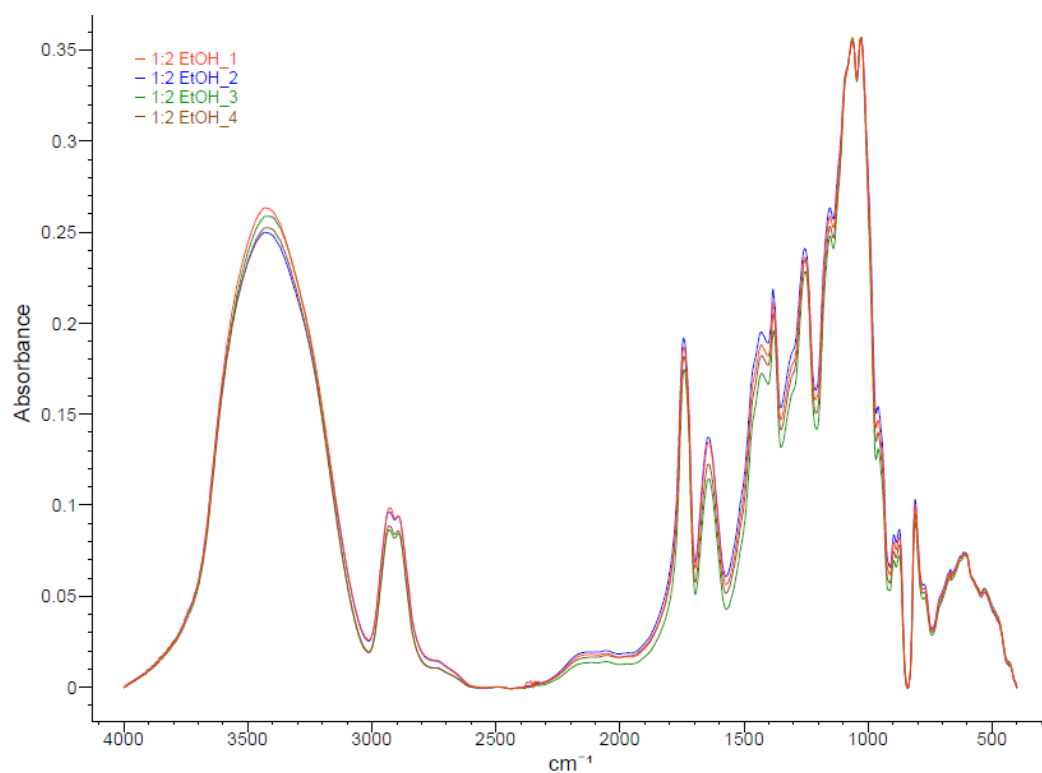


Figure B. 3. FTIR spectra for the 1:2 ethanol extracted GGM samples

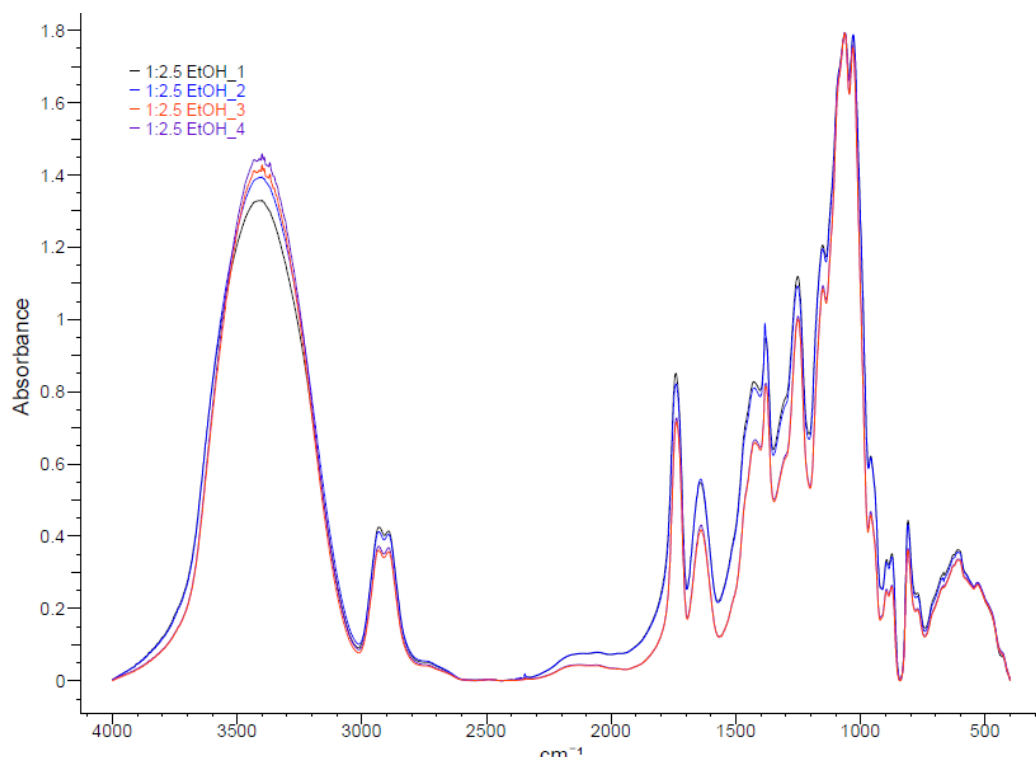


Figure B. 4. FTIR spectra for the 1:2.5 ethanol extracted GGM samples.

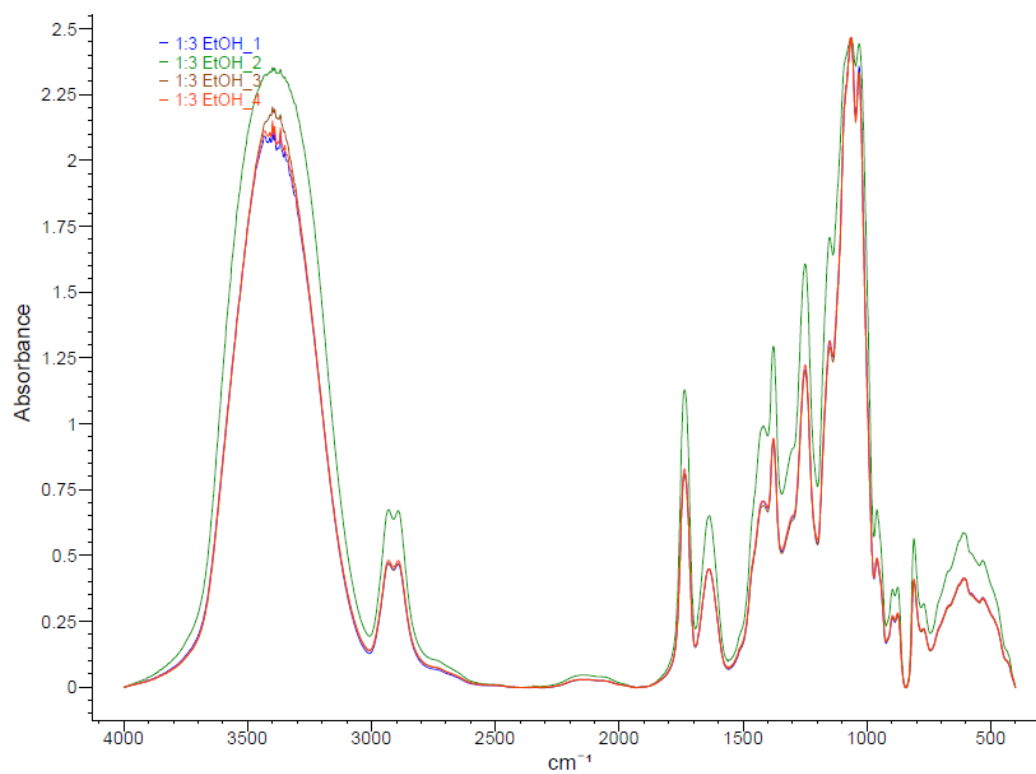


Figure B.5. FTIR spectra for the 1:3 ethanol extracted GGM samples.

B.5 DSC calculations

From the DSC analysis, the energy representing the peak in the temperature swipe of interest (-60°C to 200°C) can be used to estimate the water content. The energy representing each peak and the heat of vaporisation for water is used for calculating the water content in the samples. The calculated water mass is then compared to the total sample mass for an indication of the water content in percentage. See calculations below.

$$E_{GGM} = 845,55 \cdot 10^{-3} J$$

$$E_{GGM-DVS} = 528,11 \cdot 10^{-3} J$$

$$E_{GGM-BGE} = 201,74 \cdot 10^{-3} J$$

$$E_{GGM-DVS-BGE} = 188,95 \cdot 10^{-3} J$$

$$\Delta H_{vap}(water, 100^{\circ}C) = 2256,6 J/g$$

$$m(water)_{GGM} = \frac{E}{\Delta H_{vap}(water, 100^{\circ}C)} = \frac{845,55 \cdot 10^{-3} J}{2256,6 J/g} = 0,00037475 g = 0,37475 mg$$

$$\%water_{GGM} = \frac{m(water)}{m(sample)} = \frac{0,37475 mg}{7,95 mg} = 4,71\%$$

$$m(water)_{GGM-DVS} = 0,00023406 g = 0,23406 mg$$

$$\%water_{GGM-DVS} = \frac{0,23406 mg}{5,45 mg} = 4,29 \%$$

$$m(water)_{GGM-BGE} = 0,000089411 g = 0,08941 mg$$

$$\%water_{GGM-BGE} = \frac{0,08941 mg}{8,77 mg} = 1,02 \%$$

$$m(water)_{GGM-DVS-BGE} = 0,000083743 g = 0,083743 mg$$

$$\%water_{GGM-DVS-BGE} = \frac{0,083743 mg}{6,59 mg} = 1,27 \%$$

B.6 Result from the siphon foaming

The results from the siphon foaming experiment, including pictures for each time, are displayed in Table B.4-13 below.

Table B. 4. Siphon foaming experiment using GGM (30% (w/w)) mixed with NFC slurry (10% (w/w)). Showing the amount of the different components used and the mass used in the siphon. Since it did not foam, no mass, volume or density could be measured.

Foaming experiment: GGM-NFC	
GGM (30% (w/w))-NFC	34.29 g GGM solution + 3.77g NFC slurry
Mass volumetric flask	303.83 g
Mass in the siphon	36.53 g GGM-NFC solution
Mass after foaming	-
Volume after foaming	-
Density wet foam [g/ml]	-

Table B. 5. Siphon foaming experiment using GGM (5% (w/w)) mixed with NFC slurry (10.5% (w/w)). Showing the amount of the different components used and the mass used in the siphon, the mass and volume direct after the foaming, as well as the calculated density of the wet foam. Moreover, picture from direct after the foaming and 5 minutes later.

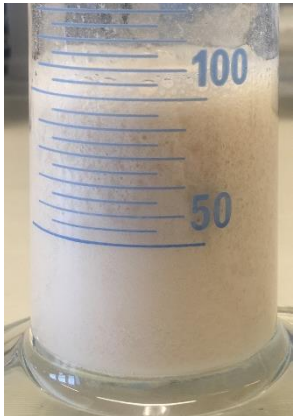
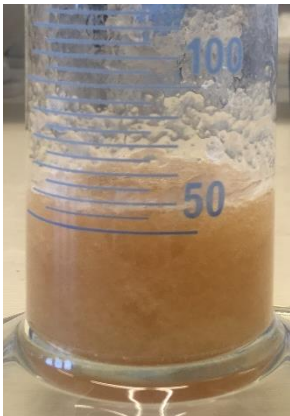
Foaming experiment: GGM-NFC	
GGM (5% (w/w))-NFC	58.52 g GGM solution + 6.89 g NFC slurry
Mass volumetric flask	303.03 g
Mass in the siphon	64.83 g GGM-NFC solution
Mass after foaming	56.94 g
Volume after foaming	105 ml
Density wet foam [g/ml]	0.5423
Picture direct:	
	
Picture 5 min later:	
	

Table B. 6. Siphon foaming experiment using GGM-BGE (5.91% (w/w)). Showing the mass of the solution used in the siphon, the mass and volume direct after the foaming, as well as the calculated density of the wet foam. Moreover, pictures from direct after the foaming, 5 minutes later, 30 minutes later and 60 minutes later.

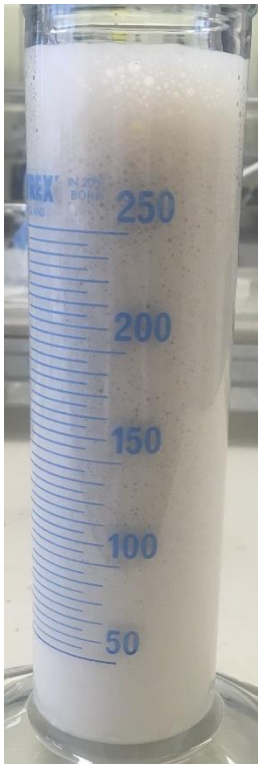



Foaming experiment: GGM-BGE			
GGM-BGE (5.91% (w/w))			
Mass volumetric flask		303.35 g	
Mass in the siphon		87.89 g GGM-BGE solution	
Mass after foaming		85.91 g	
Volume after foaming		~300 ml	
Density wet foam [g/ml]		0.2894	
Picture Direct:	Picture 5 min later:	Picture 30 min later:	Picture 60 min later:
			

Table B. 7. Siphon foaming experiment using GGM-BGE (5.91% (w/w)) mixed with NFC slurry (11% (w/w)). Showing the amount of the different components used and the mass used in the siphon, the mass and volume direct after the foaming, as well as the calculated density of the wet foam. Moreover, pictures from direct after the foaming, 5 minutes later, 30 minutes later and 60 minutes later.





Foaming experiment: GGM-BGE-NFC			
GGM-BGE (5.91% (w/w))-NFC		84.94 g GGM-BGE solution + 10.47 g NFC slurry	
Mass volumetric flask		303.78 g	
Mass in the siphon		95.16 g GGM-BGE-NFC solution	
Mass after foaming		91.61 g	
Volume after foaming		~300 ml	
Density wet foam [g/ml]		0.3054	
Picture Direct:	Picture 5 min later:	Picture 30 min later:	Picture 60 min later:
			

Table B. 8. Siphon foaming experiment using GGM-DVS (5% (w/w)). Showing the mass of the solution used in the siphon, the mass and volume direct after the foaming, as well as the calculated density of the wet foam. Moreover, pictures from direct after the foaming and 5 minutes later. No cellular structure, foam, is displayed.



Foaming experiment: GGM-DVS	
GGM (5% (w/w))-DVS	
Mass volumetric flask	303.78 g
Mass in the siphon	100.52 g GGM-DVS solution
Mass after foaming	66.24 g
Volume after foaming	~80 ml
Density wet foam [g/ml]	0.8280
Picture Direct:	Picture 5 min later:
	

Table B. 9. Siphon foaming experiment using GGM-DVS (5% (w/w)) diluted with milliQ water generating a 4.28% (w/w). Showing the mass of the different components, the mass of the solution used in the siphon, the mass and volume direct after the foaming, as well as the calculated density of the wet foam. Moreover, pictures from direct after the foaming and 5 minutes later. No cellular structure, foam, is displayed.

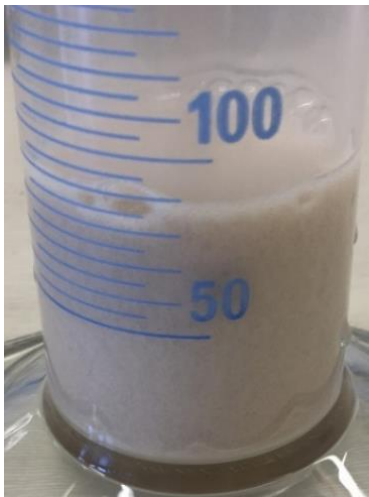
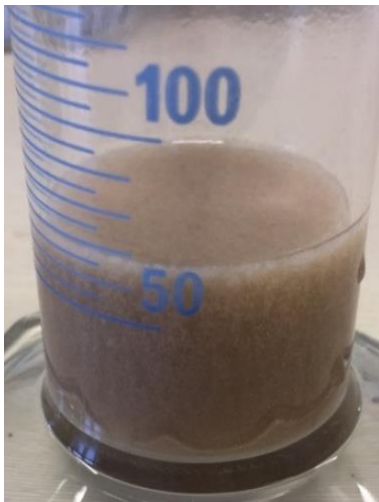
Foaming experiment: GGM DVS	
GGM (5% (w/w))-DVS	60.22 g GGM-DVS + 10 g milliQ H ₂ O
Mass volumetric flask	304.8 g
Mass in the siphon	66.94 g
Mass after foaming	62.96 g
Volume after foaming	~80 ml
Density wet foam [g/ml]	0.7870
Picture Direct:	
	
Picture 5 min later:	
	

Table B. 10. Siphon foaming experiment using GGM-DVS (4.28% (w/w)) mixed with GGM-DVS (5% (w/w)) generating a 4.32% (w/w), and the double amount of gas patrons as the other experiments. Showing the mass of the different components, the mass of the solution used in the siphon, the mass and volume direct after the foaming, as well as the calculated density of the wet foam. Moreover, pictures from direct after the foaming and 5 minutes later. No cellular structure, foam, is displayed.

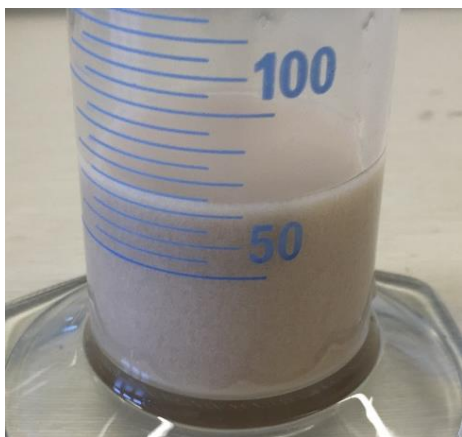
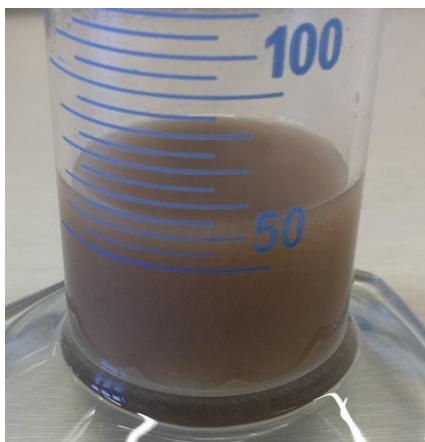
Foaming experiment: GGM-DVS	
GGM-DVS (4.28% (w/w))	61.77 g GGM-DVS (4.28% (w/w)) + 3.15 g GGM-DVS (5% (w/w))
Mass volumetric flask	303.71 g
Mass in the siphon	65.47 g GGM-DVS solution
Mass after foaming	62.38 g
Volume after foaming	~70 ml
Density wet foam [g/ml]	0.8911
Picture Direct:	Picture 5 min later:
	

Table B. 11. Siphon foaming experiment using GGM-DVS (4.32% (w/w)) mixed with NFC slurry (11% (w/w)). Showing the mass of the different components, the mass of the solution used in the siphon, the mass and volume direct after the foaming, as well as the calculated density of the wet foam. Moreover, pictures from direct after the foaming, 5 minutes later, 30 minutes later and 60 minutes later. No cellular structure, foam, is displayed.


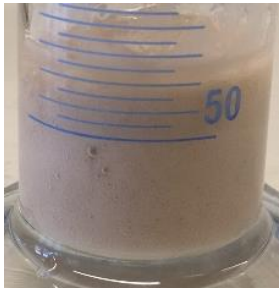


Foaming experiment: GGM-DVS-NFC			
GGM-DVS (4.32% (w/w))-NFC		55.82 g GGM-DVS solution + 6.99 g NFC slurry	
Mass volumetric flask		303.66 g	
Mass in the siphon		60.46 g GGM-DVS-NFC solution	
Mass after foaming		55.95 g	
Volume after foaming		~70 ml	
Density wet foam [g/ml]		0.7993	
Picture Direct:	Picture 5 min later:	Picture 30 min later:	Picture 60 min later:
			

Table B. 12. Siphon foaming experiment using GGM-DVS-BGE (4.79% (w/w)). Showing the mass of the solution used in the siphon, the mass and volume direct after the foaming, as well as the calculated density of the wet foam. Moreover, pictures from direct after the foaming, 5 minutes later, 30 minutes later and 60 minutes later.



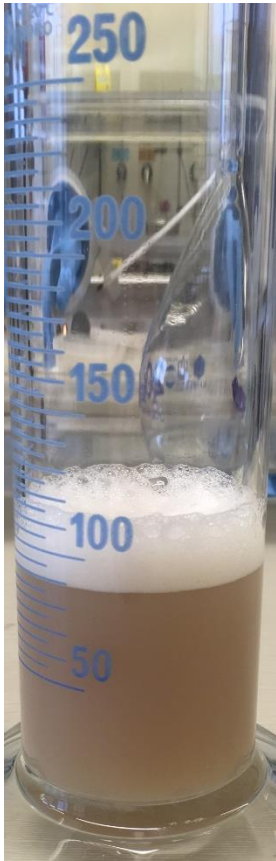

Foaming experiment: GGM-DVS-BGE			
GGM-DVS-BGE (4.79% (w/w))			
Mass volumetric flask		303.07 g	
Mass in the siphon		102.33 g GGM-DVS-BGE solution	
Mass after foaming		90.12 g	
Volume after foaming		>300 ml	
Density wet foam [g/ml]		0.3004	
Picture Direct:	Picture 5 min later:	Picture 30 min later:	Picture 60 min later:
			

Table B. 13. Siphon foaming experiment using GGM-DVS-BGE (4.79% (w/w)) mixed with NFC slurry (10% (w/w)). Showing the amount of the different components used and the mass used in the siphon, the mass and volume direct after the foaming, as well as the calculated density of the wet foam. Moreover, pictures from direct after the foaming, 5 minutes later, 30 minutes later and 60 minutes later.

Foaming experiment: GGM-DVS-BGE-NFC			
GGM-DVS-BGE (4.79% (w/w))-NFC		87.93 g GGM-DVS-BGE solution + 9.97 g NFC slurry	
Mass volumetric flask		303.64 g	
Mass in the siphon		98.88 g GGM-DVS-BGE-NFC solution	
Mass after foaming		96.02 g	
Volume after foaming		>300 ml	
Density wet foam [g/ml]		0.3201	
Picture Direct:	Picture 5 min later:	Picture 30 min later:	Picture 60 min later:
